A Historical Perspective on Lateral Collapse and Volcanic Debris Avalanches

Volcanic Debris Avalanches; from Collapse to Hazards
Springer Book Series 'Advances in Volcanology'

CHAPTER 2: A Historical Perspective on Lateral Collapse and Volcanic Debris Avalanches

Lee Siebert[1] and Matteo Roverato[2,3]

[1]Global Volcanism Program, National Museum of Natural History, Smithsonian Institution, Washington DC, USA

[2]Department of Earth Sciences, University of Geneva, Switzerland

[3]YachayTech University, School of Earth Sciences, Energy and Environment, Hacienda San José, Urcuquí, Ecuador

Abstract

In the four decades since the 1980 eruption of Mount St. Helens, debris-avalanche deposits generated by gravitational lateral collapse of volcanoes have become widely recognized. Selected regionally sequenced case studies highlight the evolution of thought regarding these events prior to 1980 in contrast to subsequent research with benefit of insights from the events of May 18, 1980. These typically hummocky deposits, of volcanic materials but lying far beyond volcanoes, had puzzled geologists for more than a century and been interpreted as a wide range of primary and secondary volcanic or non-volcanic features. Contrary to general perception, however, the volcanological literature contained multiple accounts prior to 1980 that recognized the landslide origin of some of these deposits, albeit mostly in regional publications not widely known. The burst of interest in lateral-collapse events after 1980 has led to an average of one regional or global debris-avalanche inventory annually in terrestrial or submarine settings and the recognition of a thousand events from nearly 600 volcanoes. The last major volcaniclastic process to be widely recognized and understood, large-volume debris avalanches originating from lateral collapse of volcanic edifices have been found to be a relatively common occurrence across a wide spectrum of volcanic features and settings.

Keywords

Debris avalanche, Volcaniclastic, Lateral collapse, Edifice failure, Historical review

1 Introduction.

The 1980 eruption of Mount St. Helens was one of the relatively small number of seminal events that fundamentally changed the understanding of volcanologists about volcanic processes and their deposits. The real-time and subsequent observations of what happened on the morning of May 18, 1980 (Voight et al. 1981; Glicken 1996) prompted a re-evaluation of the process of lateral collapse and the resulting generation of large-volume volcanic debris avalanches (VDAs). Subsequent work showed

that a process previously considered too rare to warrant concern in terms of volcanic hazards was a relatively common event in the life cycles of volcanoes in a wide variety of settings. The origin of volcanic debris avalanches was the last major volcaniclastic process to be widely understood and incorporated into hazard assessments, along with avalanche-generated tsunamis.

The typically hilly deposits of volcanic debris inexplicably located far beyond the flanks of volcanoes had long puzzled geologists. A wide range of both primary and secondary volcanic and non-volcanic processes had been proposed to explain their origin, but mostly commonly they were thought to be volcanic mudflows, often inferred to originate from catastrophic draining of crater lakes. Scattered references to the landslide origin of a few of these deposits in both arc and oceanic shield volcano settings had existed in the volcanic literature for more than a century (e.g. Sekiya and Kikuchi, 1889), and Japanese volcanologists in particular had recognized the similarity of hilly deposits at Bandai and other volcanoes to nonvolcanic landslides and begun to differentiate them from other types of volcanic deposits prior to 1980, although this was not widely accepted until after the Mount St. Helens collapse.

We examine selected regionally sequenced lateral-collapse events that generated large VDAs investigated prior to 1980, some well-known and others more obscure, to understand the evolution of thought about these features prior to 1980 and note later work on these deposits.

2 Regional Case Studies

2.1 Africa

Meru volcano, lying adjacent to Kilimanjaro volcano in the Gregory Rift, is cut by a 5 x 8 km depression breached to the east with a large pyroclastic cone near the headwall scarp that last erupted during the early 20th century. An extensive volcaniclastic deposit related to the breached caldera banks up against the lower flanks of Kilimanjaro as far as 60 km away. This and comparable deposits on several sides of 4565-m-high Meru volcano have been considered lahars of various ages (Downie and Wilkinson 1972; Wilkinson et al. 1983; Ghiglieri et al. 2012). The deposits on the NE to SE sides opposite Meru's large breach were mapped as one or two lahar deposits including the Momella lahar, which was thought to have formed as a result of collapse of the east flank either due to stresses associated with summit caldera subsidence resulting from magma withdrawal (Cattermole 1982) or during a major explosive eruption that formed a summit caldera that extended into a graben created by collapse of the eastern side of the volcano (Wilkinson et al. 1983, 1986).

Roberts (2002) reinterpreted the east-side deposits as resulting from lateral collapse with debris avalanche formation considered to be of tectonic origin due to the lack of associated explosive

deposits. Delcamp et al. (2016, 2017) mapped a single hummocky volcanic debris-avalanche deposit (VDAD) consisting of both the Ngare Nanyuki and Momella deposits covering an area of about 1250 km^2 with a volume of 20 ± 2 km^3 estimated from reconstruction of the pre-collapse edifice. The deposit is dominated by mixed facies material derived from the edifice. Delcamp et al. (2016) mapped two older VDADs from Meru, the intermediate Little Meru VDAD and the older Lemurge VDAD, a magmatic collapse with overlying pumice-fall and pyroclastic density current deposits, as well as deposits from more than a dozen collapse events from stratovolcanoes in this continental rift setting.

2.2 New Zealand

Taranaki Volcano (Mt. Egmont) has one of the most frequent histories of lateral collapse (Palmer and Neal 1991; Alloway et al. 2005; Zernack et al. 2012). Nevertheless, no source area scars are visible, mainly due to its cyclical re-growth (Zernack et al. 2009; Zernack and Proctor 2020 -- this volume). Thus, the hummocky topography characterized by thousands of various-size mounds located most prominently in its western sector is the only well-visible feature attributable to the multiple VDADs associated with the volcanic failures (Fig. 1). At Ruapehu, although with many fewer collapse events and large mass-flow, fluvial and tephra deposits that filled the ring plain (Hodgson 1993; Cronin and Neal 1997; Tost et al. 2014), the hummocky topography, especially in the northwestern side, is as well

preserved.

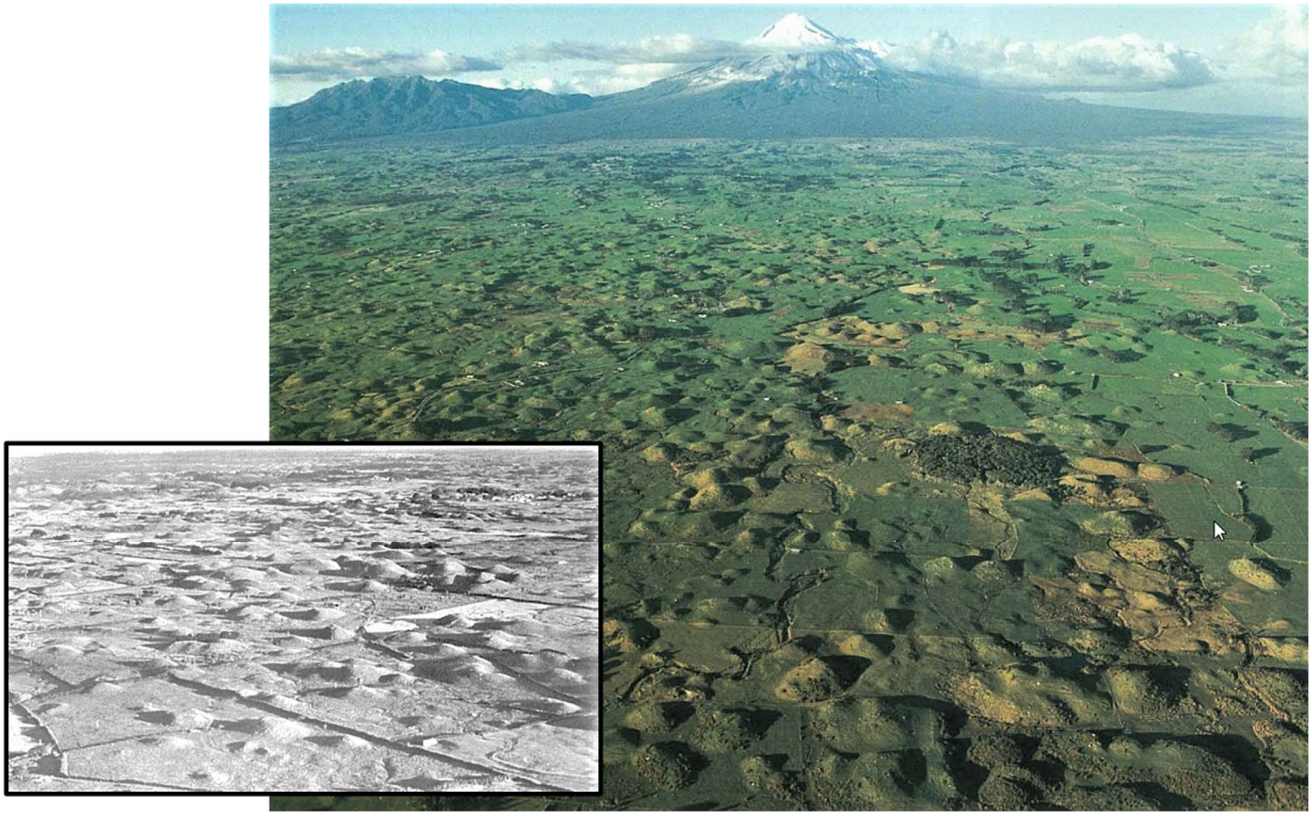

Fig 1. Taranaki volcano from the southwest with hummocky terrain dotting Taranaki's ring plain in the foreground and Pouākai volcano to the left of Taranaki. Inset: Iconic pre-1980 photograph, from the northwest, of western Taranaki "lahar mounds" landscape, showing abundant hummocks of the Pungarehu Formation (Neall 1979); photo: V.E. Neall. Color image from Malloy (1998), reproduced with permission of New Zealand Society of Soil Science.

The prevailing view of these features in New Zealand for many decades originated from a 1931 manuscript by geologist Leslie L. Grange titled "Conical Hills on Egmont and Ruapehu Volcanoes." He noted the "Conical hills, or, more correctly, dome-shaped hills," that are common on the western slopes of Mt. Egmont and on the north-west slopes of Mt. Ruapehu. Previously the western Egmont cones (a/n hummocks) have been considered as resulting from separate eruptions (Morgan and Gibson 1927) or explosions of volatiles within a lava-flow (Bossard 1928). Those on Ruapehu have been classified as blisters on a lava flow (Hill 1905) or glacial mounds (Park 1926). Grange's field studies led him to reinterpret the Taranaki and Ruapehu conical hills as "mud-flows caused either by eruption from a crater-lake, collapse of a sector of a volcano, or by the action of rain and volcanic ash on the sides of the volcanoes during or following an eruption" (Grange 1931). Furthermore, the hummocks at both

Taranaki and Ruapehu were considered analogous to the mounds topography at White Island volcano in the Bay of Plenty that just 15 years before (in 1914) formed from collapse of the northwest crater wall which transformed into a debris avalanche (mud flow for Grange) on the eastern side of the island, which killed 11 sulfur miners (Ward 1922).

At Taranaki, Neall (1979), based on field work during 1968-73 as part of his PhD thesis, together with additional field work between 1973-75, mapped several lahar deposits, some later identified as debris avalanches. Neal wrote: "they are composed almost entirely of breccia deposited by huge lahar flows that originated from the Egmont cone in the last 25,000 years [...]. About 23,000 yr BP a major explosive eruption occurred, triggering a large-scale cone collapse, and large quantities of rock, sand, and mud (over 6 km^3) swept westwards as a huge lahar to beyond the present coastline, forming the Pungarehu Formation characterized by thousands of mounds" (Fig. 1). The Pungarehu Formation is now considered a VDAD with a minimum volume of 7.5 km^3 (Alloway et al. 2005) covering an area of between 200 and 250 km^2 (Neall 1979; Ui et al. 1986; Alloway et al. 2005; Zernack et al. 2009; Roverato et al. 2015). Neall in 1974 had already recognized the Taranaki volcano as a volcanic edifice characterized by numerous destruction – re-growth cycles as confirmed later by several authors since the mid-1980s (Neall et al. 1986; Ui et al.1986; Palmer et al. 1991; Alloway et al. 2005; Procter et al. 2009; Zernack et al. 2009; Zernack et al. 2011; Zernack et al. 2012) (Fig. 2).

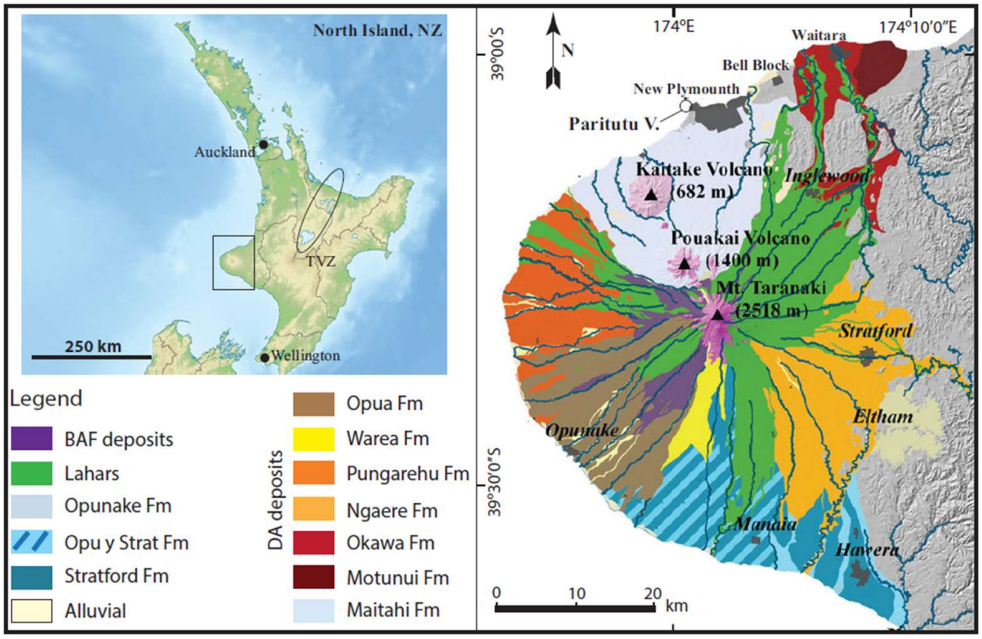

Fig. 2. Location map of the Taranaki peninsula and distribution of volcanic debris-avalanche deposits (VDADs) surrounding Taranaki volcano. TVZ—Taupo volcanic zone; BAF—block-and-ash-flow; Fm—Formation. Zernack

et al. (2012) documented 14 or more catastrophic collapses at Taranaki with volumes up to 7.5 km^3. Pleistocene Maitahi Fm VDAD originated from Pouakai, an older volcano NW of Taranaki (Gaylord et al. 2014). Figure from Roverato et al. (2015), after Zernack et al. (2011).

The origin of the large, flat-bottomed breached crater at White Island that hosts the 1914 debris-avalanche deposit has generated divergent views, most commonly as that of two or three coalescing craters. Hamilton and Baumgart (1959) originally suggested that the present crater at White Island formed by collapse of parts of the cones that characterized the island. Duncan (1970), however, argued for an origin through "explosive evacuation," while Black (1970) described the steep scar as having formed by subsidence. Clark and Cole (1986) and Cole (1986) suggested at least a partial edifice-collapse origin based on the breached crater morphology, a view discounted by Hackett and Houghton (1986) and supported by Moon et al. (2009). Variable interpretations with ambiguous evidence from bathymetry for a submarine debris-avalanche deposit were influenced by whether the Troup Head and Pinnacle Head blocks at the mouth of the breached crater (Fig. 3) are in situ remnants (Hamilton and Baumgart 1959; Thompson 1965; Cole, 1986; Hackett and Houghton 1986; Cole et al., 2000) or transported toreva blocks (Moon et al. 2009).

Fig. 3. Panoramic view of eastern end of White Island, showing in foreground conical hills formed during the 1914 collapse with Pinnacle Head (center) and Troup Head (right) blocks at mouth of breached crater (Grange 1931, photo: J. Williams).

2.3 Papua New Guinea

The 1888 collapse of Ritter island volcano off the coast of New Britain in Papua New Guinea generated the largest edifice-collapse event known in historical time. Prior to 1888, Ritter Island was a distinctively steep-sided conical stratovolcano whose summit was 780 m above sea level with a base 900 m below sea level. Several eruptions had been recorded since 1700 AD, and fumarolic activity was

continuing in 1888 with reports of vapor emission only a week prior to the collapse. On March 13, 1888, the volcano collapsed suddenly, creating a steep-sided scar about 4.4 km wide and 5 km long breached to the WNW, leaving an arcuate rim reaching only about 140 m above sea level (Fig. 4). The edifice failure created a tsunami with maximum reported wave runups of 12-15 m that reached beyond Rabaul harbor, 540 km away. Rough estimates of the number of tsunami fatalities range from 500 to 3000 (Paris et al. 2014).

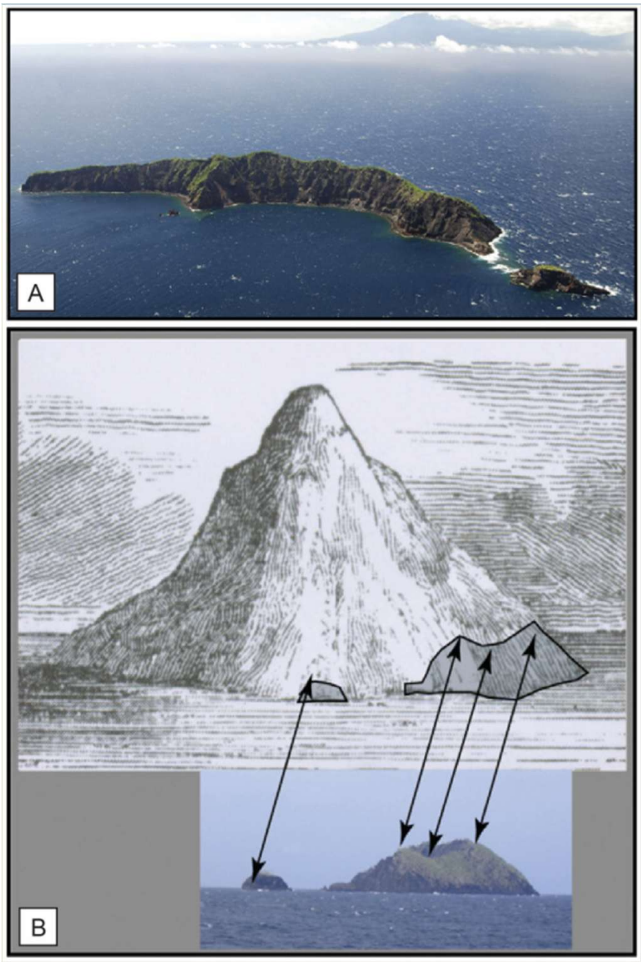

Fig. 4. Ritter Island 1888 collapse. A. Post-collapse view of Ritter Island in 2006 viewed from the southwest (photo by J. Holder). B. Sketch of Ritter Island in 1835 looking from the south (Jacobs 1844), modified with arrows correlating features on the sketch with those on post-collapse photo below. Images from Day et al. (2015).

At the time of collapse, explosion-like detonations were heard, but contemporary reports noted only a "fine, hardly noticeable ashfall" nearby (Johnson 1987, 2013). Other contemporary accounts mentioned pumice that washed up at multiple nearby beaches that could not have originated from

158 either nearby islands or distal sources and steam emissions (presumably from the sea surface)
159 immediately after the collapse (Karstens et al. 2019; Watt et al. 2019). The catastrophic destruction of
160 the volcano invited comparisons to the explosions and tsunamis of the 1888 Krakatau eruption as
161 inferred by Hammer (1907) and Taylor (1974). The Ritter Island event was likewise considered to
162 represent a major explosive eruption with climate change implications (Lamb 1970; Hoyt 1978; Pollack
163 et al. 1976; Rampino et al. 1979). The lack of evidence for major explosive activity caused Cooke
164 (1981) to rule out a Krakatau-like eruption, although he accepted a caldera subsidence origin due to
165 early bathymetric evidence describing an unbreached 2 x 3 km caldera, as did Latter (1981).

166 A bathymetric survey in 1985 revealed the breached caldera and Johnson (1987) interpreted
167 the 1888 event as a catastrophic slope failure of 4-5 km^3 of the edifice that would have generated a
168 large VDA to the west in depths below that detectable by the survey. Subsequently more detailed
169 bathymetric and high-resolution seismic surveys by Ward and Day (2003), Silver et al. (2005, 2009),
170 Day et al. (2015), Karstens et al. (2019) and Watt et al. (2019) refined the characteristics of the
171 submarine debris-avalanche deposit and related facies and tsunami generation processes.

172 High-resolution seismic surveys and sampling during a GEOMAR research cruise prompted
173 Watt et al. (2019) and Karstens et al. (2019) to recalculate the source area collapse volume downward
174 from earlier estimates to 2.4 ± 0.2 km^3 with complex associated primary and secondary mass-low facies
175 several times the volume of the original collapse. They documented a submarine depression within the
176 original edifice at 700 m depth interpreted as a syn-collapse explosion crater within which the currently
177 active post-collapse cone was constructed. The crater was attributed to a large relatively deep-water
178 bimodal explosive eruption with both a phreatic and magmatic component that may have been
179 triggered by the collapse. The eruption produced both basaltic fragments and hornblende-pumice
180 fragments with rhyolitic glass compositions.

181 **2.4 Indonesia**

182 **2.4.1 Galunggung**

183 The iconic debris-avalanche deposit of the "Ten Thousand Hills of Tasikmalaya" (Fig.5) at the
184 base of the large breached crater of Galunggung volcano in central Java caught the eye of geologists
185 dating back to Junghuhn (1853), with variable explanations for its origin. Verbeek and Fennema (1896)
186 considered that pressure from growth of a lava lake that had formed in the pre-existing breached crater
187 of Galunggung crater caused the crater walls to breach, spreading debris over the plain below. They
188 entertained several hypotheses for formation of the numerous hillocks of Tasikmalaya, including being
189 surficial expressions of explosions produced on portions of a deep-seated lava flow from draining of the

crater lava lake, but noted that the hills were mostly composed of debris from the crater walls left standing after erosional removal of finer-grained sands and gravels. They recognized that the hills were not of sufficient volume to account for the large breached crater. Most commonly, the deposit was considered to be that of a mudflow, triggered by catastrophic draining of an inferred lake in the summit crater, an interpretation motivated by comparison to frequent lahars formed by ejection of lake waters during historical eruptions of nearby Kelut volcano.

Escher (1925) mapped 3648 of these conical hills and carefully surveyed their volumes to total 0.14 km^3, a fraction of that of the missing volume of Galunggung's breached crater but noted that underlying fine and coarse debris could be considerable. Palmer (1929) in reviewing Escher's paper noted that although Escher had not specifically stated it, that the combined volume of the hillocks and the underlying material may have been equal to the missing sector of the volcano. As a source for the water needed to mobilize the mass flow, Escher postulated a large crater lake whose downslope rim was breached in part by successive vents migrating to the southeast. He considered the deposit to be intermediate between that of a mudflow and a landslide, with the hummocks (known by the Malay people as *bakoul toumpa beras* or reverse rice baskets) representing material stranded by the passing mudflow. The mudflow origin was widely adopted (e.g., Cotton 1944) and was invoked for similar hummocky terrain elsewhere.

An alternate explanation was offered by Schaffer (1926), who noted that many of the hillocks were occupied by houses and fruit trees and considered the hills to be man-made features constructed to clear flat land for rice cultivation. Schaffer pointed out several advantages of these efforts including providing refuge from passing mudflows and some degree of security from hostile marauders as well as shelter from rats and mosquitoes infesting the rice fields surrounding the hills, although he recognized that the cores of the larger hummocks were not man-made.

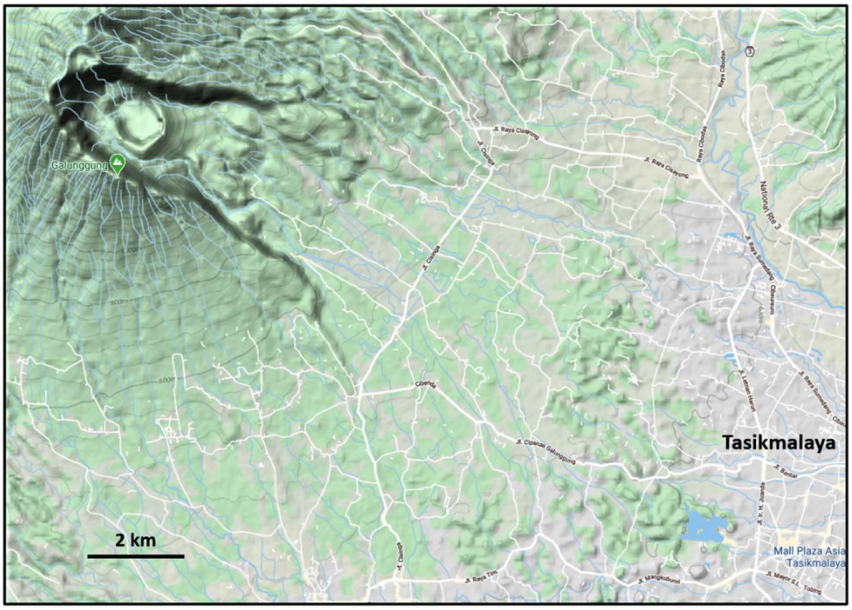

Fig. 5. Galunggung volcano with breached source area at upper left and abundant hummocks of the "Ten Thousand Hills of Tasikmalaya" below, now encroached upon by the major city of Tasikmalaya, with a population of over a million. Google Maps image.

Furuya (1978) recognized the similarities of the Galunggung deposits to those produced at Bandai in 1888 and Unzen in 1792 and considered them to be of landslide origin. Katili and Sudradjat (1984), influenced by Gorshkov's account of the 1956 Bezymianny eruption, discounted the lahar hypothesis and attributed deposits to a lateral blast, perhaps accompanied by lahars formed by crater-lake water. Juwarna et al. (1986) mapped a VDAD at Tasikmalaya and dated it at about 23,100 yr BP. Bronto (1989) dated the collapse at 4200 +/- 150 yr BP from charcoal in overlying pyroclastic-flow deposits and mapped a 170 km^2 VDAD that extends to 23 km from the active crater. Bronto (1989) calculated a total volume of ~20 km^3 for this eruption including the debris-avalanche, pyroclastic-flow, pyroclastic–surge, airfall and lahar deposits and noted that several toreva blocks remained in the breached crater.

2.4.2 Papandayan

Papandayan volcano in central Java is a complex stratovolcano with four large summit craters, the youngest of which was breached to the NE by collapse during a brief eruption in 1772 and now contains active fumarole fields. Several episodes of collapse have created an irregular profile and produced VDAs that have impacted lowland areas. The catastrophic eruption of 1772 captured the attention of Dutch geologists for more than a century, with varying interpretations of its deposits.

Eyewitness accounts reported a brief but severe eruption lasting only about five minutes near midnight on August 11-12, 1772 with an "extraordinarily bright cloud," sounds like "very heavy cannon shots" and deposits of "fire dusts and mounds of rubble" accompanying collapse of the volcano. Forty villages were in large part destroyed and 2957 persons were killed. Mohr (1773) interpreted the events of the previous year to have occurred when a large section of the volcano, including the villages, "subsided" vertically. Judd (1903) characterized the 1772 Papandayan eruption as perhaps the most violent globally during historical time, when 30 million cubic feet (~ 850,000 m^3) of materials were thrown into the atmosphere and fell around the volcano, burying 40 villages. The volcano was said to have reduced in height from 9000 to 5000 feet (from ~ 2700 to ~ 1500 m), creating a vast crater. Horsfield (1816) followed Mohr (1773) in proposing vertical subsidence. Junghuhn (1853) disputed large-scale subsidence, observing that areas beneath the volcano had increased their height by as much as 30 m and considered the crater wall to have crumbled, reducing the height of the volcano by about 300 m. He considered the breached crater to be an "explosion crater" with the destruction down valley caused by incandescent avalanches. Dutch geologist R.D.M. Verbeek, during his investigations of volcanoes in Java and Madoura (Verbeek and Fennema 1896) following his classic study of the 1883 Krakatau eruption, was intrigued by the accounts of the eruption of Papandayan more than a century earlier. Verbeek and Fennema (1896) considered the valley on the northeastern side of Papandayan to have formed when the pressure of a lava lake in the crater broke through the crater wall causing an avalanche that buried the villages, followed by a lava flow down the north flank. Taverne (1926) considered the breached crater to have existed prior to 1772. He disputed the presence of a lava lake as no fresh lava was found in the 1772 deposits and doubted that a rock avalanche would have sufficient mobility to destroy the villages. He attributed the deposits to an explosive origin, with nuées ardentes sweeping down the valley and causing the fatalities. Neumann van Padang (1929) considered that the NE crater wall, weakened by weathering, long-lasting solfataric activity, and NE-SW directed volcano-tectonic fractures, was destroyed by relatively modest phreatic explosions, causing an avalanche that destroyed the villages. He noted that six weeks after the eruption, much of the deposit could not be accessed due to underlying heat and considered the deposit to be that of a hot lahar, as appeared to be the case with Kelut volcano, where lahars retained their heat for years. Neumann van Padang (1939) later attributed the powerful block and rubble flow at Papandayan in 1772 to a landslide origin by analogy to his interpretation of the landslide at Raung volcano (see below).

Glicken et al. (1987) mapped a 0.14 km^3 clay-rich debris-avalanche deposit with few hummocks that covered 18 km^2 on the NE side of Papandayan. No deposits of a lateral blast were found. Contemporary reports of incandescence and "fire dusts" likely originated from the avalanche coming

from a high-temperature hydrothermal system at Kawah Mas, the keyhole-shaped source crater with altered, clay-rich material comparable to the lithologies found in the VDAD.

2.4.3 Raung

One of the largest debris-avalanche deposits currently known in Indonesia lies below Raung volcano in eastern Java. Gunung Gadung volcano, lying immediately west of the historically active Raung volcano, collapsed, leaving a massive 8 x 13.5 km U-shaped breached depression open to the west that was the source of a voluminous debris avalanche that created a broad area of hummocky terrain in the Jember Plain. Junghuhn (1853) considered the hilly terrain at Raung, Guntur, and Sumbing volcanoes to result from large volcanic rock streams. Kemmerling (1921) considered the hills to be pre-volcanic monadnocks on an eroded peneplain. Verbeek and Fennema (1896) described the hills as hornitos or sediment piles on the surface of a lava flow. Neumann van Padang (1939) noted the similarity of the Raung deposits to landslide deposits in Switzerland and to those at Galunggung and other Indonesian volcanoes such as Sumbing in Java and Marapi and Talakmau in Sumatra. He noted the correlation of hilly terrain in all these cases with large breached depressions in the source volcanoes and described a large avalanche deposit at Raung volcano with more than 2000 hummocks, 90% of which were under 50 m in height, that extended 60 km from its source on Gunung Gadung. Neuman van Padang attributed the mobility of the landslide to its great fall height, but also with assistance of water from draining of an inferred crater lake. The hilly terrain itself was considered to result from secondary erosional processes. Van Bemmelen (1949, 1954) likewise recognized the landslide and avalanche origin of the hummocky terrain at Raung and Galunggung volcanoes but referred to the resulting deposits as lahars.

Lukmantara (1983) attributed the deposits on the Jember Plain to mudflows, a view later supported in a hazards map by Mulyana et al. (2007), who discounted earlier interpretations as originating from a sudden landslide. A geologic map by Sutawidjaja et al. (1996) noted hummocks within the Gadung debris-avalanche deposit of varying lithologies including lava flows, pyroclastic flows and pyroclastic-fall deposits. Siebert (2002) mapped a debris-avalanche deposit that extended to about 80 km over an area of >1000 km^2 with an estimated original failure volume of 20 km^3 and an inferred deposit volume of about 25 km^3. Hummocks were found to the distal end of the deposit near the south Java coast, with distal hummocks preferentially stranded against six intervening Tertiary hill outliers and consisting dominantly of bedded pyroclastic-fall deposits. A deposit with similarities to a lateral-blast deposit locally overlies proximal parts of the avalanche deposit and a post-collapse cinder cone was constructed below the headwall scarp.

2.5 Japan

2.5.1 Bandai

One of the most noted volcanic debris-avalanche deposits world-wide prior to 1980 was that generated by the collapse of Bandai volcano in central Honshu during a phreatic eruption nearly a century earlier. Seismologist Sekiya and geologist Kikuchi of the Imperial University of Tokyo arrived at Bandai-san only a few days after the July 15, 1888 eruption and published their classic 1889 detailed account of eyewitness descriptions and observations of the deposits. The eruption began with 15-20 rapid explosions on the north flank of Ko-Bandai volcano, one of several overlapping stratovolcanoes of the Bandai volcanic complex. Eyewitnesses observed the last explosion to be projected almost horizontally northward, followed by growth of a 4-km-high vertical eruption column that produced ash fall to the Pacific coast. A pyroclastic density current swept down Biwasawa valley on the east side, but similar deposits were not widely found to the north. Failure of the summit and north flank of Ko-Bandai produced a 1.5 km^3 debris avalanche that buried several villages and traveled 11 km to the north, leaving a 1 .5 x 2 km crater breached in that direction (Fig. 6). Sekiya and Kikuchi (1889) recognized that the greater part of Ko-Bandai was not explosively ejected, but "thrown down much after the manner of a land-slip," a conclusion reinforced by their seeing the failure of a 300-m-high section of the collapse scar and the subsequent progressive disintegration of the flowing mass. The curious mound topography "like so many miniature Fujiyamas" (Fig. 6) was considered to originate from syn- and post-emplacement disintegration leaving conical shapes by forming talus aprons around them. The prominent reported explosions, however, led them to characterize the collapse scar as an *explosion crater*, noting its resemblance to the Valle del Bove at Etna and La Palma caldera in the Canary Islands, as well as to the Hoei crater formed on the flank of Fuji volcano during the 1707 eruption, the latter being an example of explosively generated craters without lateral collapse.

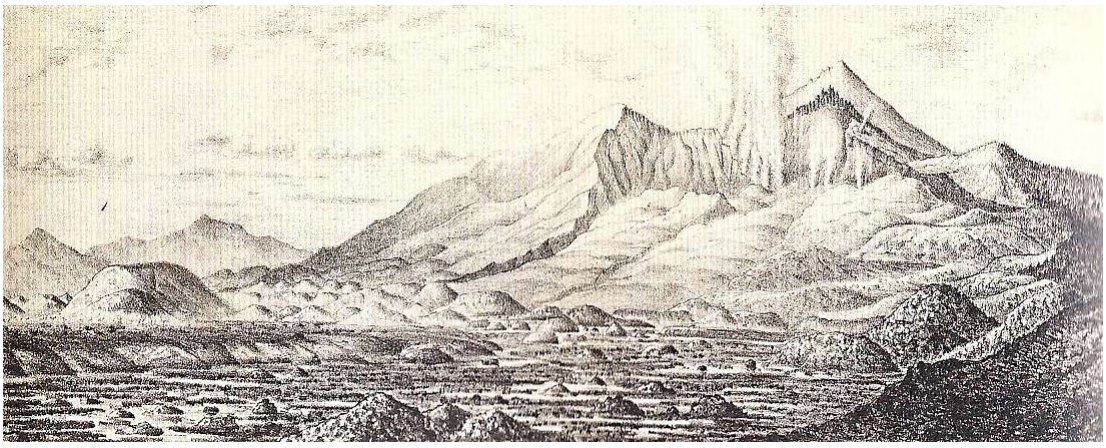

Fig. 6. Debris-avalanche hummocks of the 1888 collapse of Ko-Bandai volcano in the foreground with steam rising from fissure within source area. O-Bandai volcano lies behind peak on source area rim at right (Sekiya and Kikuchi 1889).

Subsequent investigators invoked variable mechanisms for the Bandai collapse. Koto (1916) collected avalanche debris within a few days of the eruption but considered the debris to be the result of powerful steam explosions, disagreeing with Begeat's (1900) interpretation as a landslide independent of the volcanic activity. Textbooks variably interpreted the renowned Bandai eruption. Cotton (1944) described the Bandai deposits as a water-saturated mudflow, citing Jaggar's (1930) view that the mounds represented the emplacement level of finer-grained mudflows that drained away. Rittmann (1962) considered the deposit to be that of a nuée ardente and Macdonald (1972) a volcanic mudflow transformed from an avalanche when encountering valley streams. Williams (1941) and Williams and McBirney (1979) recognized the avalanche origin of the Bandai deposits, although referring to their source as an explosion caldera.

Detailed studies of the deposits of the 1888 eruption by Nakamura (1978) noted the apparent coincidence of the avalanche with the last explosion directed to the north and concluded that although the distal portion had transformed to a mudflow, the bulk of the deposit had traveled in a dry condition and introduced the term "volcanic dry avalanche." Nakamura noted that little or no juvenile magmatic material was found in either the avalanche or air-fall tephra deposits. Moriya (1980), in his study noting the relation between hilly avalanche deposits and their breached source areas, referred to this process as *Bandaian* eruptions. Later work noted earlier collapses at the Bandai volcanic complex, including the largest known, the late-Pleistocene Okinajima VDAD on the southwest flank of the Bandai volcanic complex, which was associated with a Plinian magmatic eruption and followed by construction of O-Bandai volcano in the collapse scar (Yamamoto et al. 1999). Chiba and Kimura (2001) mapped more than 13 VDADs from Bandai volcano, most of which were smaller volume than the 1888 Urabandai VDAD and the Okinajima VDAD. Magmatic eruptions ceased at Bandai prior to eruption of the voluminous ca. 25 ka Aira-Tn tephra from the Aira caldera in Kyushu (Yamamoto et al. 1999), with Chiba and Kimura (2001) noting stratigraphic evidence for multiple magmatic collapse events at Bandai prior to eruption of the Aira-Tn tephra with subsequent collapse events associated with deposits of phreatic eruptions.

2.5.2 Yatsugatake

The late-Pleistocene Nirasaki debris-avalanche deposit from the Yatsugatake volcanic chain in central Honshu is the largest known in Japan. It extends more than 50 km from andesitic Gogen-dake

at the southern end of the chain to a wedge-shaped segment bounded by the Shiro-kawa and Kamanashi-gawa rivers above Nirasaki city and beyond. Mason and Foster (1956) considered the deposit to be a mudflow and noted varying previous interpretations. Yamasaki (1898) and Misawa (1924) also considered the deposit to be a mudflow. Misawa (1924) inferred the conical hills on the deposit to be erosional remnants from stream flow of the Kaminashi-gawa river over the deposit. Ogawa (1932) mapped the deposit as that of a piedmont glacier, describing terminal moraines and some drumlins.

Mason and Foster (1956) calculated a volume of >9.5 km^3 including distal material removed by stream erosion. They inferred that the mudflow, which may have been hot, could have originated from an earthquake or possibly Peléan eruption that produced hot avalanches, with mobility of the mudflow enhanced by steam, crater-lake waters, melting snow, or rainwater. The origin of small hills 5-20 m in height in the broad piedmont section of the deposit and larger hills in the narrow more distal wedge rising above the surface of the deposit was discussed in detail. The authors considered and rejected several hypotheses for formation of the hills, including stream erosion remnants, compressional swells, hills remaining from adjacent subsidence, or hills stranded by the momentum of the flow on bedrock, lava flows, or other topographic highs. They considered that most of the hills originated when under hydrostatic pressure of the mudflow on the volcano's slope, material of relatively low viscosity from the interior of the mudflow was extruded through fractures in the drying, hardened crust. Hashimoto et al. (1976) mapped the deposit as the Nirasaki pyroclastic flow but discussed the characteristics of mudflow hills that rose above its surface. Shortly after 1980, Mimura et al. (1982) investigated the natural remanent magnetism of the more than 100 debris-avalanche hills as high as 80 m and as wide as 500 m, previously referred to as mudflow hills. They reported that the core of the hills consisted of individual megablock material that had been rotated chiefly in the horizontal plane and rafted down slope on the relatively low temperature and dry debris avalanche.

2.5.3 Unzen

The 1792 collapse of the dacitic Mayu-yama lava dome at the Unzen volcanic complex was Japan's most severe volcanic disaster. Although phreatic explosions had often been considered to have triggered the Mayu-yama (Mae-yama) collapse, Katayama (1974) documented that no eruptions occurred at Mayu-yama. He noted the lengthy descriptions of an eruption that began on February 10, 1792 at the neighboring volcano of Fugen-dake and considered it inconceivable that residents would not have mentioned eruptive activity closer to them at Mayu-yama. On April 21, more than 300 felt earthquakes formed fissures up to 1 km long and caused extensive damage in the coastal town of

Shimabara. Loud detonations sounding to residents like guns from a Dutch frigate came from Mayu-yama, and rockfall produced dust clouds that at times obscured the mountain from Shimabara. Fear of a landslide prompted most of the residents to flee to the north, abandoning their homes. On April 29, part of the lava dome slowly slid 200 m eastward. By the middle of May, however, seismicity had subsided, and residents returned to their homes.

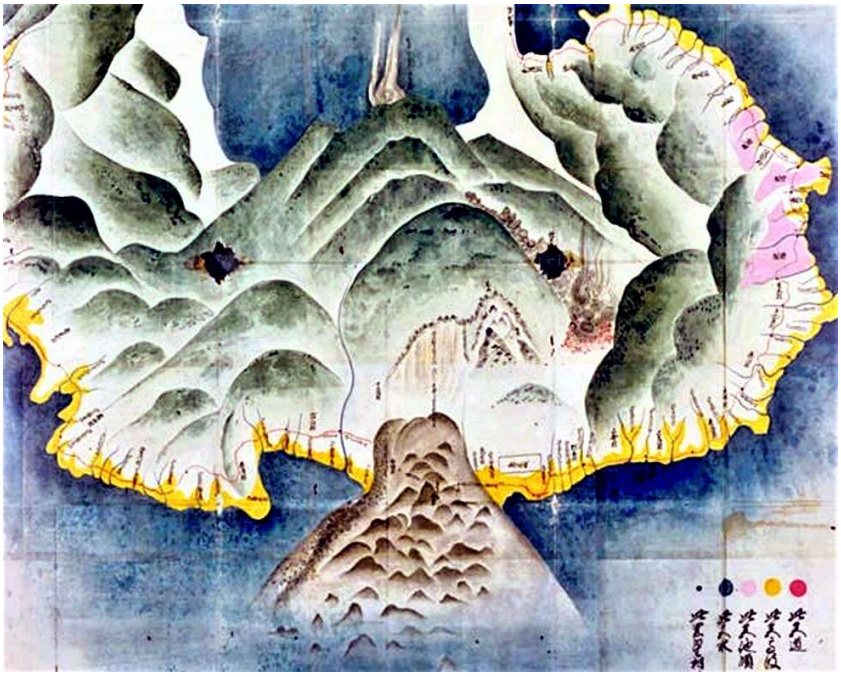

Fig. 7. Contemporary map of 1792 Unzen catastrophe. Hummocky terrain from a debris avalanche that swept into the Ariake Sea is shown in brown, with thin vertical line connecting proximal deposit area to top of the barren source area scar on Tengu-yama lava dome of Mayu-yama volcano with the twin forested Shichimenzan lava dome to right unaffected by collapse. The onshore runup of associated tsunami that swept 77 km of the Shimabara peninsula coastline is shown in yellow with red line marking coastal road. Eruptive plume rises from Fugen-dake volcano (top center) with associated flank lava flow at center right; there was no eruptive activity at the Mayu-yama dome complex. Image used with permission from Tokiwa Museum of Historical Materials, Shimabara.

At 8 p.m. on May 21, two intense earthquakes occurred, and 0.34 km^3 of Tengu-yama, the southern of the two lava domes forming Mayu-yama volcano, failed to the east; an avalanche was produced that swept into the Ariake Sea, extending the shoreline by almost 1 km and forming the Tsukumo-shima (Ninety-nine islands) (Fig. 7). A tsunami with three major wave crests swept over the most populated portion of the town and devastated a 77 km stretch of the Shimabara Peninsula coastline, causing 15,030 fatalities there and in provinces across the Ariake Sea. The landslide origin of the Mayu-yama deposits of 1792 was recognized by volcanologists in Japan prior to 1980 (e.g., Ota 1969; Furuya 1974; Katayama 1974). Hoshizumi et al. (1999) noted earlier large-volume VDAs from Nodake and Myoken-dake of the Unzen volcanic complex.

2.6 Kamchatka and Kurils

2.6.1 Bezymianny

When ash plumes subsided to allow the first post-collapse images of Mount St. Helens in 1980, the new volcano profile revealed a remarkable resemblance to Bezymianny volcano on the Kamchatka Peninsula. Subsequent studies revealed the extent to which the 1980 collapse of Mount St. Helens was virtually a carbon copy of the 1956 eruption of Bezymianny. Both eruptions were preceded by a period of crypto-dome emplacement and the onset of phreatic and/or Vulcanian eruptions lasting as long as five months at Bezymianny. Catastrophic collapse and emplacement of a major debris avalanche was accompanied by a powerful directed explosion that swept a broad arc opposite the new breached crater, blowing down trees in an aligned manner, followed by vertical Plinian explosions with pyroclastic-flow emplacement. Lava domes were subsequently emplaced in the newly formed breached craters (Fig. 8).

Gorshkov (1959, 1963) and Gorshkov and Bogoyavlenskaya (1965) detailed the development of the eruption and distinguished its deposits, although with interpretations and terminology later clarified by work on the 1980 Mount St. Helens eruption. The Bezymianny eruption and its principal deposits were considered by Gorshkov (1963) and Gorshkov and Bogoyavlenskaya (1965) to be explosively generated, characterizing them as a Bezymianny-type directed blast, with deposits of a "directed-blast agglomerate" (later shown to be that of a debris-avalanche) and a "directed-blast sand," the latter identical to deposits of the finer-grained pyroclastic-density current (often referred to as a lateral-blast deposit) at Mount St. Helens. Gorshkov's view of the Bezymianny deposits as the product of explosive eruptions was reinforced internationally in volcanological textbooks. Macdonald (1972) considered the Bezymianny eruption to be a type example of Peléean eruptions, with the explosions destroying the

whole top of the mountain and glowing avalanches descending its flanks. Bullard (1976) likewise considered the "agglomerate flow" to be an ash flow. Peter Francis, who later led ground-breaking investigations of many VDADs in South America, considered the 1956 Bezymianny eruption a modern type example of Plinian eruptions in his 1976 textbook. Williams and McBirney (1979) classified Bezymianny as a phreatic or steam blast eruption that destroyed the summit of the volcano and was followed by glowing avalanches. The interpretation of the 1956 Bezymianny deposits as explosively generated persisted in part after 1980. Melekestsev and Braitseva (1988) contrasted the deeper-seated Bezymianny crater of explosive origin to more shallow gravitational collapses at other volcanoes in Kamchatka and the Kurils.

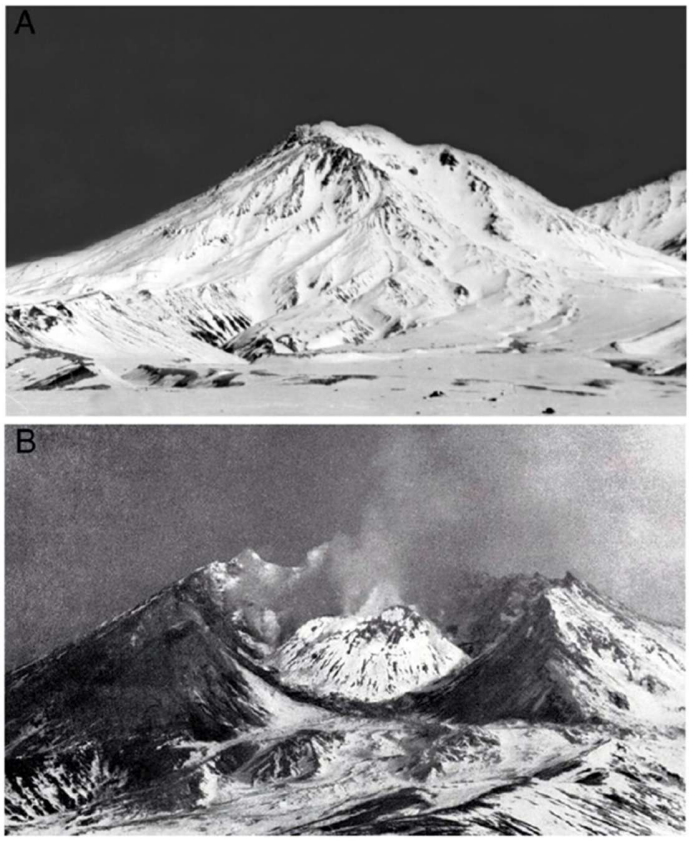

Fig. 8. Bezymianny volcano before and after 1956 collapse. A. Bezymianny volcano in 1946 (photo by B. Piip). B. Post-collapse photo in May 1957 showing new lava dome in breached depression left by 1956 collapse (photo by G. Gorshkov). Images from Girina (2013).

2.6.2 Shiveluch

A similar magmatic collapse event to that at Bezymianny took place at Shiveluch (also spelled Sheveluch) volcano in Kamchatka in 1964 (Gorshkov and Dubik 1970), although with significant differences from what occurred at Bezymianny. An earthquake at 7:07 am on November 12 triggered collapse of the edifice producing a 1.5 km^3 debris avalanche that traveled 16 km from the summit, covering an area of 98 km^2 and accompanied by minor phreatic explosions. At 7:20 am eruption of incandescent material began. A Plinian eruption column reached heights of about 15 km and continued for about an hour with the emplacement of pyroclastic flows that covered an area of about 50 km^2. The 1964 eruption was considered to be another instance of an explosively generated directed blast eruption by Gorshkov and Dubik (1970), although in contrast to at Bezymianny, only deposits of the "lateral-blast agglomerate" were identified. Belousov (1995) attributed the lack of a "directed-blast sand" deposit to the absence of magma high in the edifice at the time of failure, with depressurization of the hydrothermal system in the upper edifice not being sufficient to trigger a magmatic pyroclastic density current (lateral-blast) eruption. Large-scale lateral collapse was not unprecedented at Shiveluch; Ponomareva et al. (1998) and Belousov et al. (1999) documented eight or more collapse events at Shiveluch during the Holocene. All of the eight events documented by Belousov et al. (1999) were comparable to the 1964 eruption in that failure occurred prior to magma reaching the upper edifice and directed-blast deposits were not documented.

The Bezymianny, Shiveluch, and Mount St. Helens eruptions were instructive in the understanding of collapse events at volcanoes. Voight et al. (1981) in their work on the 1980 Mount St. Helens deposit and Ui (1983) and Siebert (1984) in assessing global analogs, noted the similarity of accounts of the 1956 Bezymianny and 1964 "directed-blast agglomerate" deposits to that of the Mount St. Helens debris-avalanche deposit. Ryabinin and Rodionov (1966) earlier had calculated that the Bezymianny edifice could not have contained sufficient steam to produce its 1956 crater, and Adushkin et al. (1984) showed that the 1956 airwaves were inconsistent with a blast of that size. Post-1980 field studies of the 1956 Bezymianny (Bogoyavlenskaya et al. 1985; Belousov and Belousova 1998) and 1964 Shiveluch deposits (Bogoyavlenskaya et al. 1985; Belousov 1995; Ponomareva et al. 1998) detailed their rockslide-debris avalanche origin. Belousov et al. (1999, 2007) noted distinctions between magmatic collapse events contingent on the location of magma within the edifice at the time of failure, with the absence of a directed-blast deposit at Shiveluch due to the lack of magma high in the edifice at the time of collapse, in contrast to conditions at Bezymianny and Mount St. Helens.

2.6.3 Kharimkotan

Gorshkov (1970) extended the interpretation of lateral-collapse events as explosively generated directed blasts in Kamchatka to large breached craters in Kuril Islands volcanoes such as Kharimkotan (Harimkotan). A large VDA during the 1933 eruption of Kharimkotan (also known as Severgin) that extended the shoreline by a kilometer and generated a tsunami (Fig. 9) was interpreted by Miyatake (1934) as a mudflow. The collapse was followed by Plinian eruptions that produced pyroclastic flows, but Belousov et al. (2007) considered magma to have been relatively deep beneath the summit at the time of collapse as the VDAD contained little juvenile material and, as at Shiveluch volcano in 1964, a lateral-blast deposit comparable to that at Mount St. Helens was not found. Five or more large VDAs were documented at Kharimkotan during the Holocene, including one to the east about 1100 yr BP and another to the northwest about 2000 yr BP that was also followed by Plinian eruptions (Belousova and Belousov 1995; Belousov and Belousova 1996).

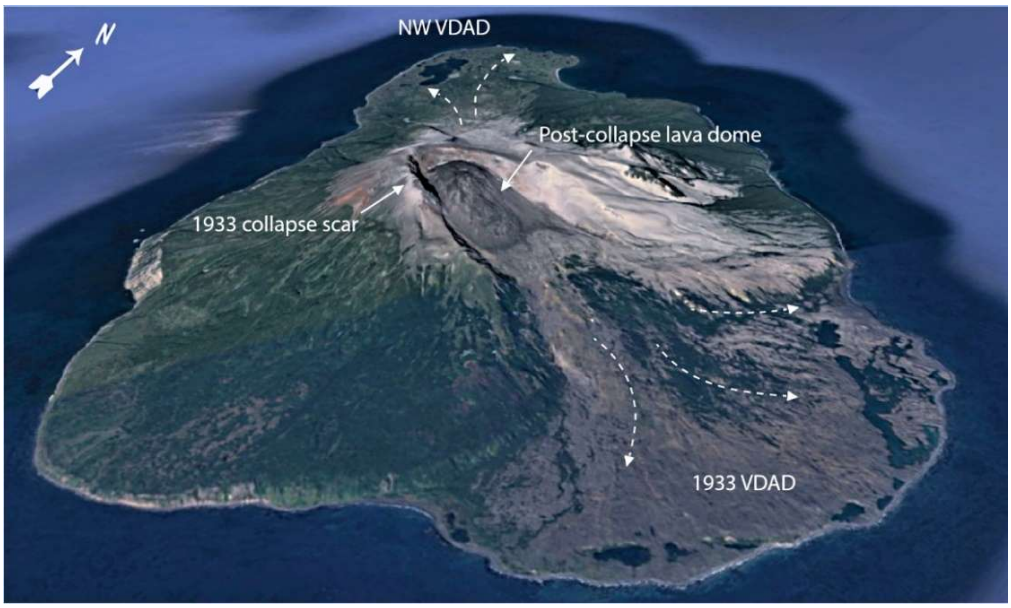

Fig. 9. Kharimkotan (Harimkotan) volcano showing volcanic debris-avalanche deposits (VDADs). White arrows show direction of avalanche movement. The debris avalanches entered the sea, with the 1933 avalanche extending the shoreline and producing a tsunami that caused two fatalities on a neighboring island (Belousova and Belousov 1995). Other Holocene debris avalanches include one about 1100 yr BP on the east side underlying the 1933 VDAD and another at about 2000 yr BP on the northwestern side (Belousov and Belousova 1996). Modified from 2006 Google Earth image.

2.7 Alaska and Cascade Range

508 ### 2.7.1 Mageik

509 Robert F. Griggs was a University of Ohio botanist working on studies of kelp off the coast of the
510 Alaska Peninsula in 1913 when he noticed the effect of ash from the seminal 1912 eruption of
511 Novarupta (Katmai) on Kodiak Island vegetation. He was thrust into the role of dealing with a major
512 geological event when during a multi-year grant from the National Geographic Society he discovered in
513 1916 the awe-inspiring Valley of Ten Thousand Smokes ignimbrite deposit near Katmai volcano. During
514 his Katmai investigations Griggs encountered another puzzling deposit on the flanks of Mageik volcano
515 that he considered of almost comparable interest to the Katmai crater and the Valley of Ten Thousand
516 Smokes (Griggs, 1920, 1922). In 1917 Griggs observed a massive chaotic deposit in the upper reaches
517 of Martin Creek on the south side of Mageik volcano consisting of jumbled, fragmented rock of
518 dominantly volcanic origin, but also containing sandstone blocks and segments of soil and plant
519 remains. Many rock boulders were more than 10 m in maximum size, and the surface of the deposit
520 contained numerous conical mounds and small ponds (Fig. 10).

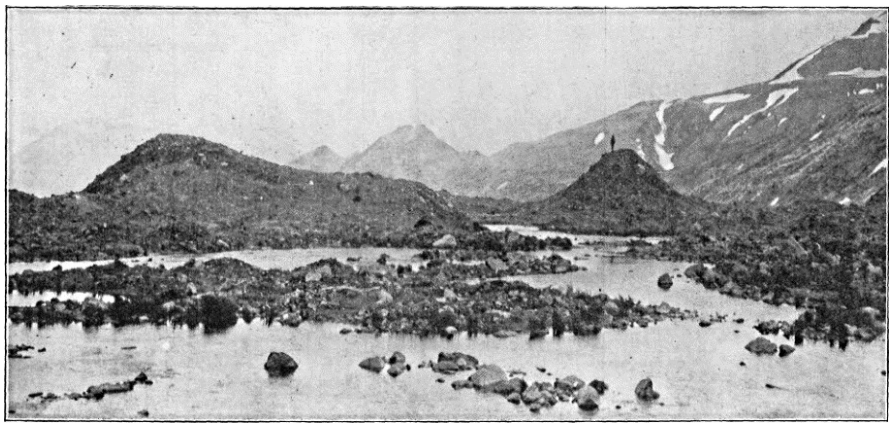

521

522 Fig. 10. Conical hummock (right) of Mageik debris-avalanche deposit in 1917 with person standing on top for
523 scale and flowing stream not yet incised through the 1912 avalanche deposit (Griggs 1920).

524

525 Griggs initially considered the Mageik deposit to be of glacial origin, noting the many circular
526 ponds similar to kettle ponds on glaciers, but evidence of its sudden emplacement and morphological
527 similarities to non-volcanic landslide deposits and that at Bandai volcano in Japan led to his
528 interpretation of the deposit as originating from a landslide on the flank of Mageik volcano. He
529 discussed the origin of the mounds in some detail, noting that they had not previously been adequately
530 described and concluded that they were characteristic features of large landslide deposits. The
531 presence of Katmai (Novarupta) ash on the surface of the deposit and the lack of decay of entrained

vegetation led him to consider the landslide to be contemporaneous with the 1912 eruption. Griggs calculated the volume of the deposit to be about 0.9 km^3, assuming a conservative average thickness of about 10 yards (~ 9 m). Hildreth et al. (2000) mapped three VDADs originating from Mageik, the largest of which was about 0.35 km^3 in volume. They noted that part of Griggs' 1912 deposit was that of an older avalanche and estimated a volume of 0.05-0.1 km^3 for the 1912 debris-avalanche deposit.

2.7.2 Augustine

Prior to his work on the Mageik landslide deposit as part of his Katmai investigations, Griggs had briefly stopped at Augustine Island in Cook Inlet in 1913 during the first year of his Alaska studies (Griggs 1920, 1922). He observed the hummocky terrain at Burr Point on the northeast side of the island and later considered it as an analogue for his interpretation of the Mageik landslide deposit and others in the Katmai area. The latest debris avalanche at uninhabited Augustine volcano took place in 1883. Contemporary accounts (Dall 1884; Davidson 1884) focused primarily on observations of eruption plumes and a tsunami that swept across Cook Inlet, but also noted a ship captain's observations that "from the summit a great slide of the mountain over half a mile broad had taken place towards the rocky boat harbor on the north-northwestward." A geologic map of Augustine Island (Detterman 1973) considered parts of VDADs on the east, south, and northeast coasts to be in-situ lava flows but recognized "volcanic rubble flows" and mudflow deposits elsewhere. Kienle and Forbes (1976) attributed deposits and tsunami generation of the 1883 eruption to mudflows and nuées ardentes. Kienle and Swanson (1980) attributed flank hazards at Augustine mostly to lahars and pyroclastic flows entering the sea, which they revised in a 1983 hazard assessment to note the presence of VDADs. The brief reference of Griggs (1920) to a landslide deposit on Augustine was in a paper on Mageik volcano, and it wasn't until after 1980 that the debris-avalanche origin of widespread deposits at Augustine was recognized. Siebert et al. (1989, 1995) studied the 1883 Burr Point deposit and the larger West Island VDAD on the NW side and noted bathymetric evidence for other debris avalanches on all sides of the island. Begét and Kienle (1992) and Waitt and Begét (2009) expanded work on Augustine to investigate the extensive debris-avalanche deposits that ringed Augustine volcano. At least a dozen large VDAs were found to have occurred within the past 2500 years, making Augustine the volcano with the highest-known frequency of edifice-failure debris avalanches (Fig. 11).

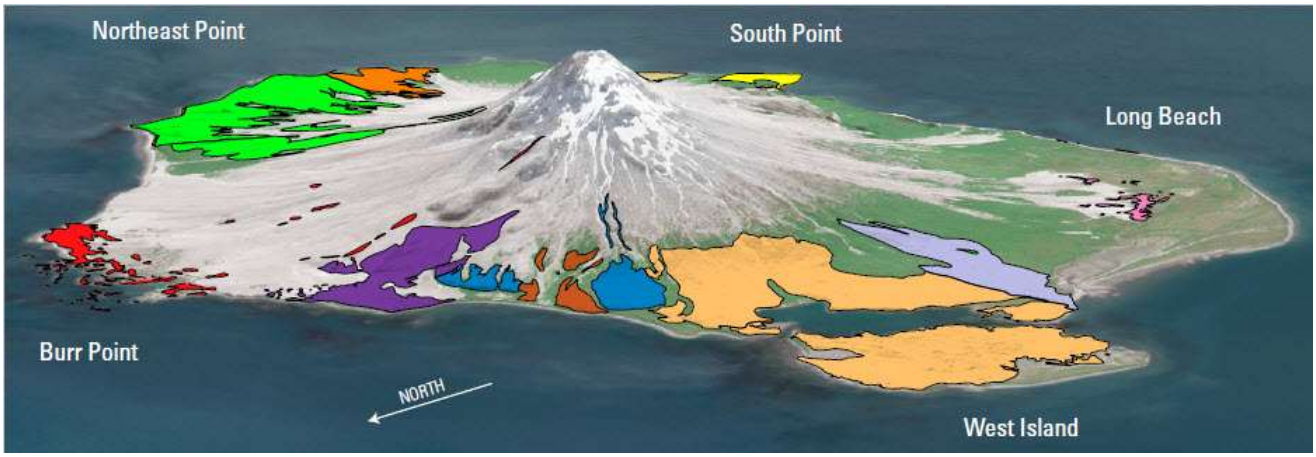

Fig. 11. Augustine volcano has collapsed a dozen times or more in the past 2,500 years. Debris-avalanche deposits in this image extend out to sea on all sides and are variably covered by deposits of younger eruptions closer to the volcano. Selected deposits are named, with the 1883 AD Burr Point deposit (in red) being the youngest. VDADs mapped by Waitt and Begét (2009) are overlaid on July 3, 2018 Landsat 8 imagery.

2.7.3 Shasta

The hilly topography of the massive VDA from Shasta volcano in northern California, the largest Quaternary debris avalanche known in the western U.S., puzzled geologists for more than a half century. Its origin remained a mystery until after the 1980 eruption of Mount St. Helens, when Harry Glicken and other USGS volcanologists driving across the extensive deposit on Interstate-5 highway to and from destinations in California from the Cascade Volcano Observatory noted its resemblance to what they had been working on at Mount St. Helens (Fig. 12). Crandell (1989) noted an impressive array of previous interpretations for the deposit. Diller et al. (1915) had considered the hills of lava and tuff to originate at least in part from minor local eruptions that pierced Cretaceous bedrock, forming small volcanic deposits around individual vents. Fenner (1923) proposed that a shallow sill had been intruded beneath Shasta Valley, with small bodies of magma breaching the surface to form the hills. Williams (1949) and later Mack (1960) and Hotz (1977) mapped the proximal part of the deposit as glacial moraines originating from a glacier on the northwestern slopes of the volcano and flat-lying areas between hummocks as fluvioglacial outwash. Distal portions were described as Tertiary Western Cascade lavas and tuff breccias with intervening alluvium, with hillocks representing erosional remnants.

Fig. 12. Hummocks of Shasta Valley debris-avalanche deposit with Shasta volcano in the background. Large feature on right horizon is not a hummock, but Holocene Black Butte lava dome. Photo: Stephen Brantley.

Christiansen (1982) briefly noted the presence of a large debris-avalanche deposit in the Shasta Valley, and the deposit was studied in detail by Crandell et al. (1984) and Crandell (1989). Crandell (1989) mapped a deposit that covered at least 675 km^2 with a volume of 45 km^3 or more that was emplaced between about 300,000 and 380,000 years ago. The northern terminus of the hilly block facies lies about 49 km from the present summit of the volcano, with intervening flat areas of matrix facies, consisting of unsorted and unstratified mudflow-like deposits chiefly from the volcano. Shasta displays some of the largest hummocks of subaerial debris avalanches, with some reaching more than a kilometer in length. Analysis of hummock dimensions (Herrick et al. 2013) showed that Shasta hummocks displayed the same logarithmic decay in hummock size with distance from the source that was apparent in data sets with the smallest-diameter hummocks as longer travel distances provided more time for disaggregation of block-facies hummock material (Fig. 13).

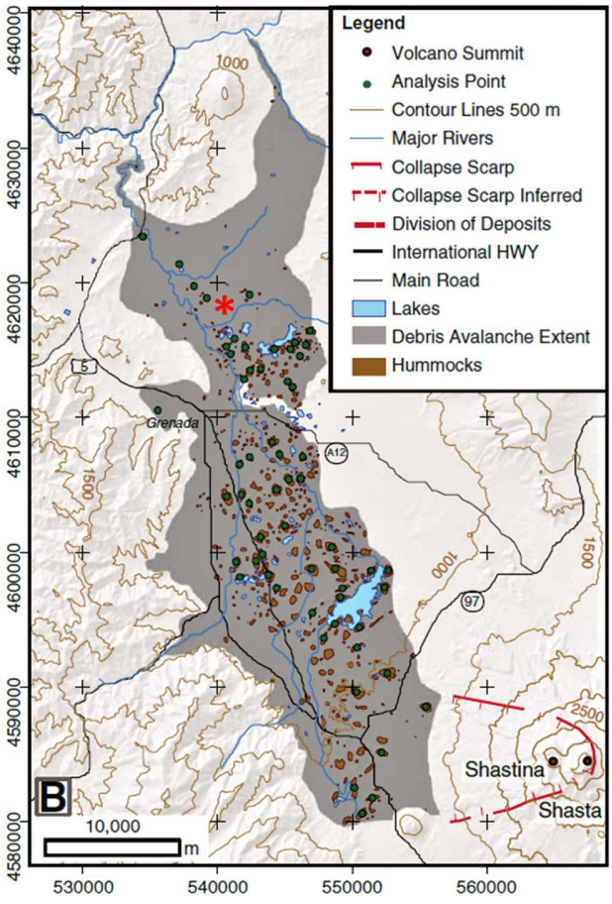

Fig. 13. Map of 487 larger-size hummocks of Shasta Valley VDAD with red dashed line showing inferred source area (Herrick et al. 2013) and red asterisk marking location of Fig. 12 photo.

2.7.4 Chaos Crags

A much smaller debris-avalanche deposit (0.15 km^3) at Chaos Crags lava-dome complex in the Lassen volcanic center of northern California was recognized by Williams (1928), Heath (1960) and Crandell et al. (1974) as a rockfall-avalanche deposit. Williams (1928) considered the avalanche to have required a basal wet component that moved as a mudflow to explain its great mobility. Heath (1960) considered the three discrete lobes of the deposit to have been emplaced during separate events spanning as much as 1200 years, although Crandell et al. (1974) documented evidence for a single retrogressive failure that took place about 300 years ago and calculated a minimum velocity of

160 km/hr based on runup of 120 m of the distal part of the avalanche on to the flanks of Table Mountain. Eppler et al. (1987) modeled avalanche kinematics with respect to potential hazards impacting a Lassen National Park road and visitor center constructed on the deposit and concluded that a future avalanche would be of smaller size given the reduced volume of the dome and potential to reach the road but not visitor facilities.

2.8 Mexico

Colima Volcano is considered the most active volcano in Mexico and is also known as Volcán de Fuego (*Fire Volcano*). The volcano was built on the southern flank of the older Nevado de Colima volcano, and inside the Paleofuego depression, a 4-km-wide relic of a Holocene lateral collapse (Robin et al. 1987; Luhr and Prestegaard, 1988). This depression has been interpreted in different ways since the beginning of the last century. Waitz (1906) was the first to write about the origin of the scar of Colima volcano, considering it as a *maar* and defending his ideas over the next decades (Waitz 1932). Mooser (1961), on the other hand, defined the scar as a "submergence caldera" and hypothesized that the depression was generated by multiple phases of magma-chamber collapse. Mooser also described, for the first time, two other "calderas" of the neighboring Nevado de Colima volcano. The same hypothesis was supported by Luhr and Carmichael (1980), who defined these depressions as summit calderas likely formed by the collapse of shallow magma chambers. One year before, Demant (1979) considered the theories of Waitz (1906, 1932) as inconsistent with a *maar* formation and suggested, instead, that the depression of Colima volcano had formed through cyclical violent ash and pumice eruptions. In 1978 the Instituto Nacional de Estatística, Geografia y Informática (National Institute of Statistics and Geography) started a geological survey of Mexico, resulting in a series of geological maps of Colima volcano and surrounding areas (INEGI, 1984). In these maps, the VDADs cropping out in the volcano ring-plain were considered as volcanic breccias.

In the early 1980s, the "caldera" of Colima volcano was finally recognized to be a debris avalanche-related collapse scar (Luhr and Carmichael 1982; Robin et al. 1984). Several years later, Robin et al. (1987) and Luhr and Prestegaard (1988) described the collapse event in detail and the associated debris avalanche as a single, broad deposit although with divergent ages of 9370±400 yr BP and 4280±110 yr BP, respectively. A geomorphology study (Hubp et al. 1993) of the Colima area describes the hummocky topography in the SE and SW Colima volcano ring plain as possibly related to two distinct VDADs, using the Robin/Luhr's age divergence to support their idea.

The Colima volcanic complex is now known to have a complex stratigraphy of collapse events, with several Pleistocene events at ancestral Nevado de Colima volcano (Cortes et al. 2010) and as

many as eight major deposits from Paleofuego and the historically active Volcán de Fuego volcanoes during the past 30,000 years, the most recent of which was the 2500 yr BP El Remate-Armería VDAD (Stoopes and Sheridan 1992; Komorowski et al. 1997; Capra et al. 2002; Cortes et al. 2005; Cortes et al. 2010; Roverato et al. 2011, Roverato and Capra 2013; Cortes et al. 2019).

2.9 South America

2.9.1 Chimborazo

Massive 6263-m Chimborazo volcano, Ecuador's highest peak, has undergone a major collapse event that remained unrecognized until the late 1980s. Deposits of the largest Chimborazo collapse underlie the city of Riobamba, part of a VDA (Riobamba Formation) that travelled more than 40 km to the southeast (Alcaraz 2002; Bernard et al. 2008) (Fig. 14). In the early 1980s the Riobamba VDAD was considered a lahar deposit caused by an eruption of Chimborazo inferred to be during or shortly after the last glaciation (Clapperton 1983). The remnant of the collapse scar is still slightly visible in the northwestern volcanic flank, although later volcanic activity and glacial erosion have obliterated most of it. Kilian (1987) and Kilian et al. (1995) described the scar as a subsidence caldera, although no associated ignimbrite deposits have been found, and defined the Riobamba formation as generic volcanic debris. Beginning in the late 1980s several authors recognized the edifice collapse and associated VDAD (Beate and Hall 1989; Clapperton 1990, Beate et al. 1990), although there have been differing views regarding which of the edifices of the Chimborazo volcanic complex sourced the avalanche and the age of collapse. Barba et al. (2005) and Samianego et al. (2012) used geochemical comparisons of edifice and deposit rocks and avalanche deposit size considerations to propose that the collapse originated from the basal CH-I edifice about 60-65 ka and that the three current summits post-date the avalanche with the previously hypothesized subsidence caldera scar originating from the debris-avalanche event. The first detailed studies of the Riobamba VDAD by Alcaraz (2002) and Bernard et al. (2008) showed that the avalanche deposit covers an area of about 280 km^2 with an estimated volume of >11 km^3 (Bernard et al. 2008), making it one of the largest known in Ecuador. The Riobamba VDAD is dominated by block facies material, although the relatively small size of larger blocks (<5 m^2) suggests cataclasis at or near the source (Bernard et al. 2008). Samaniego et al. (2012) also mapped a smaller Río Colorado VDAD on the north flank emplaced about 12-24 ka that originated from the CH-III Young Cone edifice.

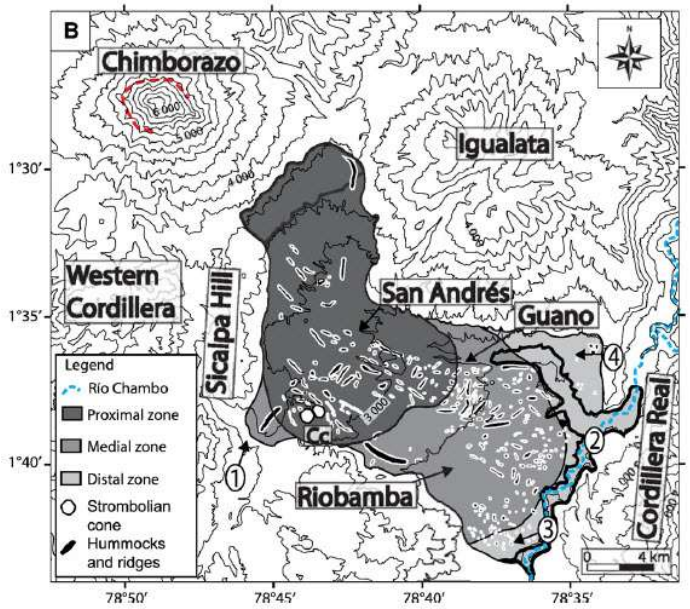

Fig. 14. Map of Riobamba VDAD from Chimborazo volcano with dashed red line marking inferred source area from collapse of basal CH-I edifice. Image from Bernard et al. (2008).

2.9.2 San Pedro

San Pedro volcano in the Atacama region is considered one of the largest, highest and most recently active volcanoes in northern Chile (Francis and Wells, 1988). The volcano displays a collapse scar and a VDAD in its northern ring plain, which was one of the first to be recognized in the Andes during a survey by Francis et al. (1974) (Fig. 15). The authors described several "hot" deposits that they considered to be of nuées ardentes that extended up to 20 km from the source. They noted that some avalanches were polylithologic and unlikely to be due to the collapse of hot lava bodies and that some of the extensive debris flows which are found on the lower slopes of San Pedro likely were of the older cone. Some of the proximal hot avalanches were likely produced by the collapse of some summit domes related to the post-failure re-growth of San Pedro volcano and were unrelated to the main collapse scar.

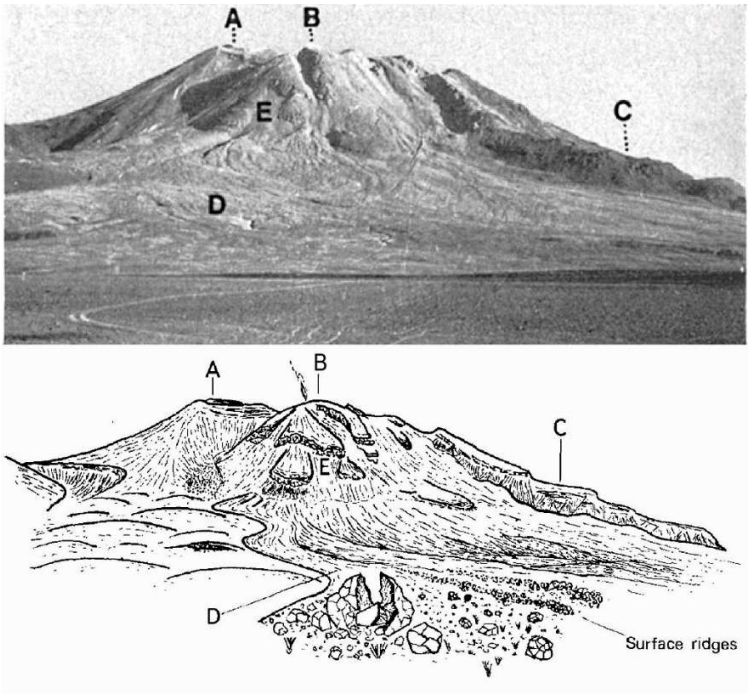

Fig. 15. Photo and sketch of San Pedro volcano from the northwest. A – main, eastern summit, B – younger, western cone, C – thick andesite lava, D – extensive apron of hot avalanche deposits, E– prominent collapse scar above D. Image from Francis et al. (1974).

The distal outcrops described as polylithologic and as debris flows are likely the distal "hybrid" facies of a broad debris-avalanche body. A decade later, O'Callaghan and Francis (1986) interpreted the collapse event and the associated VDAD as comparable to that at Mount St. Helens a few years before and recognized the distal debris flow deposits as facies of a major VDAD.

2.9.3 Socompa

A massive debris avalanche from Socompa volcano covered about 500 km^2 of the Atacama Desert of the northern Chilean Andes about 7200 years ago and is one of earth's best exposed major debris-avalanche deposits. The first to recognize the avalanche as a major phenomenon was Bruggen (1942), who interpreted the deposit as some form of glacial moraine. Deruelle (1978) considered the "Negros de Aras deposits" to be that of a pumiceous nuée ardente partly covered with lava blocks from the destroyed northwestern quadrant of Socompa Volcano, a not unreasonable conclusion at the time due to widespread pumiceous pyroclastic-flow deposits, later shown to be derived from substrate ignimbrites of the Salin Formation. Deruelle did correlate the deposit with the well-visible summit scar,

706 but he considered the scar a "real caldera," referring to a subsidence caldera with the nuée ardente
707 being the associated ignimbrite.
708 Francis et al. (1985) recognized the debris-avalanche origin of the extensive Socompa deposits.
709 Glassy, breadcrust and prismatically jointed blocks (evidence of hot cracking that would not have
710 survived cold transport) are evidence of a possible hot lava dome (Francis et al. 1985) or hot lava flow
711 (Wadge et al. 1995) at the time of collapse, although the failure plane cut deep into pre-Socompa
712 substrate. The Socompa deposit is noted for its massive kilometer-scale toreva blocks within and at the
713 base of the source scar, which is partially filled by post-collapse dacitic lava domes, lava flows and
714 pyroclastic-flow deposits. Its pristine stage of preservation in the arid Atacama desert facilitated both
715 field and remote sensing analysis that has led to its becoming one of the world's most extensively
716 studied volcanic debris avalanches, leading to better understanding of the deposit and collapse
717 dynamics (Francis et al. 1985; Francis and Wells 1988; Ramirez 1988; Wadge et al. 1995; van Wyk de
718 Vries et al. 2001; Kelfoun and Druitt 2005; Kelfoun et al. 2008; Shea and van Wyk de Vries 2008;
719 Davies et al. 2010).

720 **2.9.4 Tata Sabaya**

721 Following his 1978 interpretation of nuées ardentes at Socompa volcano, Deruelle and Brousse
722 (1984) noted in that other nuée ardente deposits had been discovered in the central Andes at the base
723 of the Tata Sabaya volcano in southern Bolivia near the Chilean border. Deruelle and Brousse (1984)
724 described the nuée ardente as a broad pumice flow that was emitted from the SE flank of the volcano
725 with a runout of at least 20 km and reported prismatically jointed blocks scattered on the surface of the
726 deposit. A year later Francis and Ramirez (1985) re-interpreted the deposit from morphological
727 evidence as that of a large debris-avalanche deposit analogous to that at Mount St. Helens and
728 Socompa volcanoes. They noted, as a chief diagnostic feature, the extensive hummocky topography
729 with numerous small hills and depressions, prominent in satellite imagery due to emplacement over
730 light-colored deposits of the Salar de Coipasa. The prismatic jointed blocks that are described by
731 Deruelle and Brousse (1984) are typical of "hot avalanche" deposits indicating magmatic activity at the
732 time of or after the collapse (Francis and Ramirez 1985). The first detailed field study of the deposit was
733 by de Silva et al. (1993), who described the collapse scar, well visible in the northern sector of the
734 volcano, the extension and volume of the VDAD, and its morphology with hummocky topography and
735 toreva blocks located in the upper part of the edifice. Godoy et al. (2012) discussed six different
736 hummock facies of the 6-8 km^3 VDAD covering an area of about 230 km^2 (Fig. 16) that permitted
737 inferences about the pre-collapse structure of the edifice and avalanche emplacement.

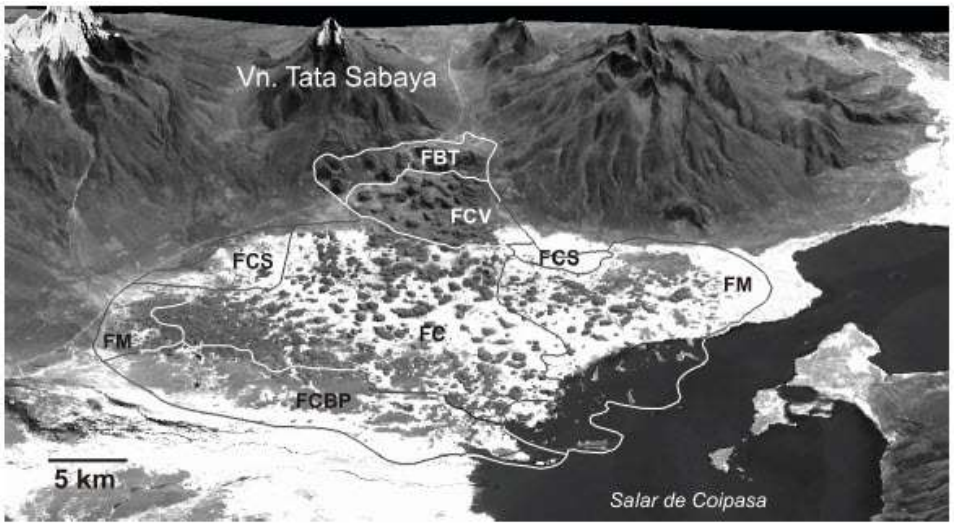

Fig. 16. Oblique perspective with unspecified vertical exaggeration (Godoy et al. 2012) of Tata Sabaya volcano and its 6-8 km^3 debris-avalanche deposit extending as far as 23 km into the Salar de Coipasa. Labeled hummock facies are discussed in Godoy et al. (2012).

2.10 Submarine debris-avalanche deposits from oceanic shield volcanoes

Large-scale collapse of oceanic shield volcanoes had received relatively little attention until the onset of detailed bathymetric studies that identified large-scale submarine debris-avalanche deposits. The massive source regions of these collapses, common in island chains such as the Hawaiian and Canary Islands, had typically been interpreted as either of erosional or tectonic origin or due to caldera collapse associated with major explosive eruptions. Major sea cliffs truncating several of the Hawaiian Islands were generally considered to originate from faulting or wave erosion (Stearns 1946; Macdonald and Abbott 1970). Early interpretations of bathymetric studies of submarine deposits off the southern Hawaiian ridge considered them to be seamounts (Hamilton, 1957). Moore (1964) recognized these deposits as originating from massive submarine landslides from Ko'olau (Oahu) and Molokai, although this view was disputed (e.g. Langford and Brill 1972) until the advent of comprehensive sonar surveys of the entire Hawaiian Islands in the late 1980s (Moore et al. 1989, 1994) (Fig. 17). Volcano instability processes in the Hawaiian Islands are evaluated in detail by Denlinger and Morgan (2014).

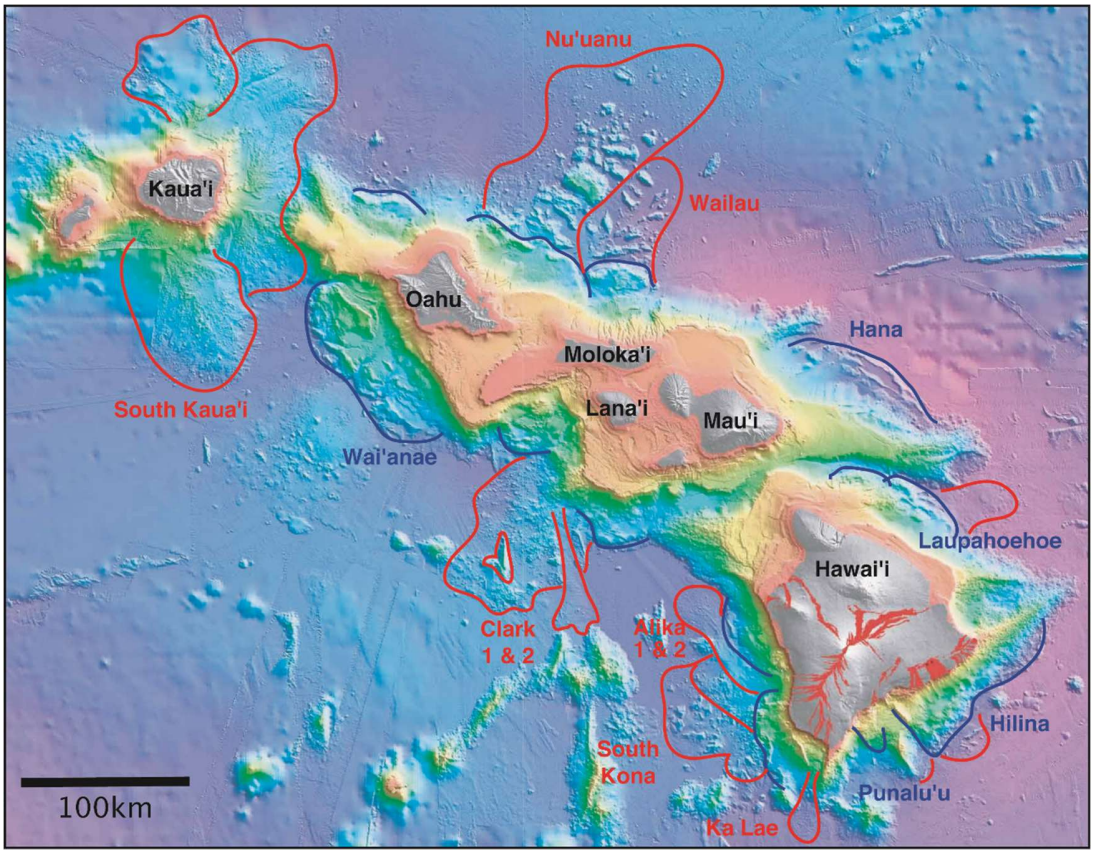

Fig. 17. Landslides and slumps around the Hawaiian Islands. The submarine landslide deposits off the northern coasts of Oahu and Molokai Islands were identified by Moore (1964) from bathymetry, an interpretation expanded on by detailed side-looking sonar surveys of the Hawaiian island chain and Hawaiian Ridge in the 1980s. Red lines and labels mark submarine debris-avalanche deposits and blue lines and labels mark slumps from Moore et al. (1989, 1994), supplemented by work of T. Sisson and Morgan et al. (2009). Bathymetry from Eakins et al. (2004). Image courtesy J. Morgan.

The remarkable landslide scars on Tenerife and other Canary Islands volcanoes long attracted the attention of geologists and generated considerable controversy, particularly regarding the origin of the Las Cañadas caldera on Tenerife as summarized by Martí (2019). Pre-1980 interpretations of the origin of Las Cañadas caldera largely considered it to be of explosive origin with associated vertical caldera collapse, although Bravo (1962) and Coello (1973) proposed a landslide origin. Post-1980 views of the formation of the complex Las Cañadas summit depression and the contiguous Icod valley extending to the coast included explosive vertical caldera collapse, landslide origin, or a combination of the two.

772 Elsewhere on Tenerife volcano Rothpletz (1889) noted the similarity of the Orotava valley to the
773 Valle de Bove on Etna volcano and considered them to originate from explosive eruptions, as did Wolf
774 (1931) and Hausen (1956). Fritsch and Reiss (1868) considered Orotava valley to have formed from a
775 combination of lava accumulation and fluvial erosion, as did Benitez Padilla (1946), Fuster et al. (1968),
776 and Palacios (1994), who noted the absence of submarine landslide deposits. The landslide origin
777 hypothesis dates back to von Buch (1825), who considered that large masses of volcanic material had
778 slid into the sea, leaving the Orotava depression. Bravo (1962), Hausen (1970) and Coello (1973)
779 supported the landslide origin, along with at other Canary Islands volcanoes such as El Hierro (Hausen,
780 1969) and La Palma (Hausen, 1973). These views gained widespread acceptance with the discovery of
781 bathymetric evidence for massive submarine landslide deposits beginning in the early 1990s, as
782 summarized in regional reviews of Canary Islands landslides in Table 1 and accompanying references.
783 A profusion of bathymetric studies of island chains in the Pacific, Atlantic, and Indian Oceans has
784 demonstrated the proclivity of collapse of oceanic shield volcanoes with extremely large collapse
785 volumes associated with related to their massive edifice sizes (Table 1).

786 ## 3 Post-1980 research

787 Although there had been some degree of understanding of lateral edifice-failure events
788 prior to the 1980 collapse at Mount St. Helens, they were not widely known. The scientific attention
789 focused on the dramatic events of the May 18 collapse triggered a major reevaluation of similar
790 deposits elsewhere and a recognition of their significant volcanic hazards implications. This is reflected
791 in an average of more than one global or regional inventory of lateral edifice failure and debris-
792 avalanche occurrence a year in the four decades since 1980, including a significant number concerning
793 submarine VDADs from failure of oceanic shield volcanoes (Table 1; see more discussion in Dufresne
794 et al. 2020a - this volume). This interest in lateral-collapse phenomena was accompanied by wide-
795 ranging efforts to understand the still controversial mechanisms involved (Paguican et al. 2020 - this
796 volume). A thousand lateral-collapse events have now been identified from nearly 600 volcanoes in
797 varied geological settings from debris-avalanche deposits and inferred source areas (Table 1). The vast
798 majority of these are Quaternary in age, but VDADs have been identified as far back as the
799 Precambrian (Trofimovs et al. 2004; Roverato 2016).

800

Region	Cases	References	Region	Cases	References
Tanzania	14	Delcamp et al. (2016)	**Guatemala**	17	Vallance et al. (1995)
New Zealand	14	Palmer et al. (1991)	**Central America**	42	Siebert et al. (2006)

New Zealand	10	Neall (2002)	**Ecuador**	29	Andrade (2009)
Papua New Guinea	21	Johnson (1987)	**Ecuador**	46	Bernard and Andrade (2019)
Papua New Guinea	12	Silver et al. (2009)	**Central Andes**	42	Francis and Wells (1988)
Indonesia	70	MacLeod (1989)	**West Indies**	6	Deplus et al. (2001)
Japan	71	Ui et al. (1986)	**West Indies**	47	Boudon et al. (2007)
Japan	>100	Inokuchi (1988)	**Madeira Is**	8	Quartau et al. (2018)
Japan-Hokkaido	13	Yamagishi (1996)	**Canary Is**	15	Krastel et al. (2001)
Japan	128	Inokuchi (2006)	**Canary Is**	11	Masson et al. (2002)
Japan	67	Yoshida (2016)	**Canary Is**	26	Acosta et al. (2004)
Kurile Is	>40	Belousova and Belousov (2011)	**Canary Is**	31	Hunt et al. (2014)
Kamchatka and Kurils	13	Melekestsev and Braitseva (1988)	**Cape Verde Is**	8	Masson et al. (2008)
Kamchatka	33	Ponomareva et al. (2006)	**Global**	43	Ui (1983)
Aleutian Is	14	Coombs et al. (2007)	**Global**	97	Siebert (1984)
Aleutian Is	17	Montanero and Beget (2011)	**Global**	195	Siebert et al. (1987)
Cascade Range	48	Siebert and Vallance (2017)	**Global**	56	Holcomb and Searle (1991)
Hawaiian Is	11	Moore et al. (1989)	**Global (Rift islands)**	20	Mitchell (2003)
Hawaiian Is	20	McMurtry et al. (2004)	**Global**	316	Dufresne et al. (2008)
Hawaiian Ridge	>68	Moore et al. (1994)	**Global**	301	Bernard (2008)
Society and Austral Is	13	Clouard and Bonneville (2004)	**Global**	182	Blahůt et al. (2019)
Mexico	23	Capra et al. (2002)	**Global**	1001	This study; Dufresne et al. (2020)

Table 1. Regional and global VDAD inventories with number of reported cases. Submarine event totals exclude debris flows or low-velocity slumps. Blue color indicates inventories with largely submarine deposits. See Dufresne et al. (2020a - this volume) for chronologically sequenced list with additional context.

Recent collapse events >0.1 km^3 in volume have averaged more than 5 per century since 1500 AD and about 7 per century since 1800 AD (Table 2). Comparable events with volumes <0.1 km^3, such as those at White Island in New Zealand in 1914 (Grange, 1931), Soufrière Hills on Montserrat in 1997 (Voight et al. 2002) and the catastrophic Casita collapse in Nicaragua in 1998 (Scott et al. 2005) are not included here. More than three-quarters of these tabulated recent collapse events are associated with magmatic eruptions, although contrary to common perception, lateral blasts such as occurred at Mount St. Helens in 1980 and Bezymianny in 1956 have been identified with only a few others (Table 2). This is consistent with lateral-blast generation requiring the precise coincidence of collapse at the time of explosions, typically when a magma body is high in the edifice and collapsing slide blocks deflect decompression-generated explosions (Belousov et al. 1999, 2007; Siebert 2002). When magma is farther below the summit, collapse can be completed before the onset of magmatic eruptions, leaving an open vent resulting in more typical vertical explosions, as occurred at Shiveluch volcano in 1964.

Volcano	Location	Type	Year	km^3	km^2	Fatal	Agent	Type	VEI	References
Anak Krakatau	Indonesia	Stratovolcano	**2018**	(0.27)	-	>437	T	M	3	Grilli et al. (2019)
Bawakaraeng	Indonesia	Stratovolcano	**2004**	0.2	-	32	A	-	-	Tsuchiya et al. (2009)
Fernandina	Galapagos	Caldera	**1988**	0.9	10	-	-	M	2	Chadwick et al. (1991)
St. Helens	Cascades	Stratovolcano	**1980**	2.5	64	57	P,A,L	Mb	5	Voight et al. (1981)
Shiveluch	Kamchatka	Dome	**1964**	1.5	98	-	-	M	4	Gorshkov and Dubik (1970)
Bezymianny	Kamchatka	Stratovolcano	**1956**	0.8	30	-	-	Mb	5	Gorshkov (1959)
Kharimkotan	Kurile Is	Dome	**1933**	0.5	>20	2	T	M	5	Belousova and Belousov (1995)
Hakuba-Oike	Japan	Compound	**1911**	0.15	-	-	-	-	-	Yoshida (2016)
Ritter Island	Melanesia	Stratovolcano	**1888**	(2.4-4.2)	100	3000?	T	M	2?	Johnson (1987)
Bandai	Japan	Stratovolcano	**1888**	1.5	34	461	A,P	P	4	Sekiya and Kikuchi (1889)
Augustine	Alaska	Dome	**1883**	0.3	21	-	-	M	4	Siebert et al. (1995)
Krakatau	Indonesia	Stratovolcano	**1883**	(<<3.8)	-	(?)	T,P	M	5	Camus et al. (1992)
Sinarka	Kurile Is	Stratovolcano	**1878**	0.5?	-	?	A	M	4	Belousova and Belousov (2011)
Tate-yama	Japan	Stratovolcano	**1858**	0.2	-	Many	-	-	-	Nozaki (2015)
Suwanose-jima	Japan	Stratovolcano	**1813**	>1.0	-	-	-	M	4	Shimano et al. (2013)
Tutupaca	Peru	Stratovolcano	**1802?**	0.7?	-	-	-	M	4?	Samaniego et al. (2015)
Unzen	Japan	Dome	**1792**	0.34	15	15,030	T,A	-	-	Ota (1969)
Asama	Japan	Stratovolcano	**1783**	0.14	n/d	1491?	A,P,L	M	4	Tamura and Hayakawa (1995)
Papandayan	Indonesia	Stratovolcano	**1772**	0.14	18	2957	A	P	3	Glicken et al. (1987)
Oshima-Oshima	Japan	Stratovolcano	**1741**	2.5	69	1475	T	M	4	Satake and Kate (2001)
Augustine	Alaska	Dome	**1700?**	0.15	10	-	-	M	?	Siebert et al. (1995)
Nabukelevu	Fiji	Dome	**1650?**	>0.1?	-	-	-	M	?	Cronin et al. (2004)
Callaqui	Chile	Stratovolcano	**1630?**	<0.7	-	-	-	M	?	Polanco and Naranjo (2008)
Chaos Crags	Cascades	Dome	**1650?**	0.15	8	-	-	-	-	Crandell et al. (1974)
Komagatake	Japan	Stratovolcano	**1640**	1.55	176	700	T	Mb	5	Yoshimoto and Ui (1998)
Ruiz	Colombia	Stratovolcano	**1595**	>0.5	-	636	L	M	4	Thouret et al. (1990)
Augustine	Alaska	Dome	**1540?**	0.5	30	-	-	Mb	4?	Siebert et al. (1995)
Rainier	Cascades	Stratovolcano	**1500?**	0.23	-	-	-	-	-	Scott et al. (2001)

817

818 Table 2. Debris avalanches ≥0.1 km^3 since 1500 AD, some of which are flank failures that did not involve the
819 central core of the volcano. Volumes in parentheses are source area volumes. Fatality agents: A, avalanche; L,
820 lahar; P, pyroclastic density current; T, tsunami. Known tsunami fatalities at Krakatau in 1883 are not listed
821 because, although large-volume submarine debris-avalanche deposits have been identified (Camus et al. 1992;
822 Deplus et al. 1995), the number of potential related tsunami fatalities is not known. Type of collapse: M, magmatic
823 eruptions; Mb, magmatic eruption with lateral blast; P, phreatic eruption. At Unzen volcano in 1792 there was no
824 eruption at the Mayu-yama dome complex where collapse occurred although there was at neighboring Fugen-
825 dake volcano (Fig 2.7). VEI: Volcanic Explosivity Index (Newhall and Self 1982). Single reference for each deposit

focuses on early work pertaining to edifice collapse; additional references can be found in text of selected case studies.

When magma is even deeper, phreatic eruptions where no juvenile magma reaches the surface can occur, as at Bandai in 1888.

Alternatively, failure can occur in the absence of eruptive activity, as in about a fifth of the events tabulated here. This degree of magmatic involvement cannot be extrapolated to older events, however, as associated eruptive activity is documented for only a small fraction of earlier collapse events (Dufresne et al. 2020a - this volume). It should be noted that of collapses an order of magnitude smaller in volume than those documented in Table 2 during this same 500-year interval, more than half were non-eruptive events.

Fatalities are known to have occurred at more than half of these events listed in Table 2 and would have occurred at many more had they not occurred in uninhabited or sparsely populated regions. The total number is strongly dominated by the debris-avalanche induced tsunamis during the Mayu-yama collapse at Unzen volcano in 1792. These numbers could be substantially higher depending on the uncertain degree of tsunami generation associated with an apparent debris-avalanche component of the 1883 Krakatau eruption (Camus et al. 1992; Deplus et al. 1995). This type of tsunami hazard was recently underscored by the collapse of Anak Krakatau in December 2018 during early stages of work on this volume (Grilli et al. 2019).

4 Discussion

4.1 Deposits

The generation and emplacement of lateral edifice-collapse debris avalanches has been the last mechanism of large-scale edifice destruction and subsequent volcaniclastic processes to be widely recognized and understood. These deposits of often hilly volcanic material located far beyond the volcanoes themselves had long puzzled geologists. Deposits at the smaller end of the size spectrum of large VDAs (<1 km^3), such as those from White Island in New Zealand in 1914, Mageik and Augustine in Alaska, and Chaos Crags in the Cascade Range were more readily recognized by some as landslide or rockfall avalanches prior to 1980, but with some exceptions, such as for some Indonesian and Canary Islands volcanoes, it remained difficult to comprehend that this process could be responsible on much more massive scales. The previous discussion of individual collapse events highlights the wide variation in pre-1980 interpretations, with both primary and secondary volcanic processes and non-volcanic processes invoked (Table 3).

857

Origin	Volcanoes
Primary/secondary volcanic processes/deposits	
Lava flows	Taranaki, Ruapehu, Papandayan (1772), Galunggung, Raung, Augustine, Shasta
Secondary explosions from lava flows	Taranaki, Galunggung, Raung
Sill intrusion with pockets of surficial magma	Shasta
Individual volcanic vents	Taranaki, Shasta, Ko'olau, Molokai
Explosive eruptions	Meru, Taranaki, Ruapehu, Ritter Island (1888), Papandayan (1772), Yatsugatake, Bandai (1888), Colima, Chimborazo, Tenerife
Laterally directed explosions	Galunggung, Bezymianny (1956), Shiveluch (1964), Kharimkotan (1933)
Pyroclastic flows	Papandayan (1772), Yatsugatake, Bandai (1888), Bezymianny (1956), Augustine, Shasta, San Pedro, Socompa, Tata Sabaya
Lahars	Meru, Taranaki, Ruapehu, White Island (1914), Papandayan (1772), Galunggung, Raung, Yatsugatake, Bandai (1888), Kharimkotan (1933), Augustine, Chimborazo, San Pedro
Landslides/debris avalanches	Talakmau, Marapi, Guntur, Papandayan (1772), Galunggung, Sumbing, Raung, Unzen (1792), Bandai (1888), Mageik (1912), Augustine, Chaos Crags, Ko'olau, Molokai, Tenerife, La Palma, El Hierro
Non-volcanic processes/deposits	
Erosional processes	Talakmau, Marapi, Galunggung, Sumbing, Raung, Yatsugatake, Shasta
Pre-volcanic erosion (monadnocks)	Raung
Glacial deposits	Ruapehu, Yatsugatake, Shasta, Socompa
Anthropogenic	Galunggung
Source areas	
Explosive eruptions	Papandayan (1772), Bandai (1888), Bezymianny (1956), Shiveluch (1964), Kharimkotan (1933), Colima, Tenerife
Maar formation	Colima
Caldera collapse: magma chamber evacuation	Meru, Ritter Island (1888), Colima, Socompa, Tenerife
Trap-door caldera	Tenerife, La Palma, El Hierro
Subsidence (mostly non-eruptive)	Meru, Ritter Island (1888), Papandayan (1772), Chimborazo
Faulting	Ko'olau, Molokai
Erosional processes (fluvial, wave erosion)	Ko'olau, Molokai, Tenerife
Landslides/debris avalanches	Talakmau, Marapi, Galunggung, Sumbing, Raung, Unzen, Bandai (1888), Chaos Crags, Ko'olau, Molokai, Tenerife, La Palma, El Hierro

858

859 Table 3

Pre-1980 interpretations of deposits and source areas of landslide/debris avalanche events (with a few post-1980 interpretations prior to or after recognition as edifice collapse events). Associated volcanoes are those discussed in the text.

Primary mechanisms included the interpretation of the deposits as individual volcanic vents or those of lava flows or pyroclastic flows. Variations of lava-flow origins included interpretations as primary lava flows, "blisters" or hornitos on the surface of a lava flow, or explosions of volatiles within the lava flow. The hilly deposits had also been considered at Shasta volcano to result from the intrusion of sills beneath valley floors from which individual pockets of magma breached the surface. The 1956 Bezymianny and 1964 Shiveluch eruptions in Kamchatka prompted interpretations of debris-avalanche deposits to be the products of powerful laterally directed explosions.

Secondary processes invoked included interpretation of the hilly terrain as erosional remnants of volcanic topography. Most often they were considered of glacial or mudflow (lahar) origin, although one view of the Ten Thousand Hills of Tasikmalaya at Galunggung volcano in Java was that they were of anthropogenic origin. Surface morphology features such as shallow ponds and lateral levees similar to the kettle ponds and lateral moraines at glaciers influenced interpretations as volcanic material redistributed by glaciers. Most commonly, the deposits were thought to be those of mudflows, a natural outcome of the textural similarities of homogenized mixed facies material to that of lahar deposits. The massive amounts of water needed to saturate these deposits prompted many to invoke the failure of the rim of a summit crater lake. This inferred origin was influenced by the many lahars produced during explosive ejection of crater lake waters at Kelut volcano in Indonesia. Debris-avalanche hummocks were often referred to as mudflow hills, flow mounds, or lahar mounds, reflecting the perceived view of water-saturated emplacement.

Although the 1980 eruption of Mount St. Helens was a watershed event that changed the understanding of lateral-collapse events, contrary to popular perception there had already been recognition of the landslide origin of some of these events dating back to the 19th century, as at Bandai volcano in 1888 (Sekiya and Kikuchi, 1889). Robert F. Griggs, a botanist thrust into a geologic role in documenting the 1912 Katmai-Novarupa eruption, published an early insightful analysis of the morphological and textural similarity of hilly deposits at volcanoes in Alaska to those of non-volcanic landslides (Griggs 1920). Volcanologists in Indonesia attributed the formation of massive deposits at Raung and other volcanoes to high-velocity avalanches (Junghuhn 1853; Neumann van Padang 1939; van Bemmelen 1949). Von Buch (1825), Bravo (1962), Moore (1964), Hausen (1969,1970, 1973), and

Coello (1973) described the landslide origin of massive scars on Canary Islands and Hawaiian volcanoes. It is worth noting that in the relatively small number of samples discussed here, there were more volcanoes where deposits were recognized to be of landslide origin than those of lahar origin (Table 3), despite the preponderance of the latter view in the volcanological community prior to 1980.

In the years prior to 1980 volcanologists in Japan began deposit-based differentiation of avalanche deposits from mudflow deposits. Murai (1961), in a study of pyroclastic flows in Japan, used the term "dry mud-flow" to distinguish deposits that were previously characterized as mudflows, such as those from Bandai volcano in 1888, but were avalanches caused by collapse of part of the volcanic cone emplaced by "gravitational forces without the agency of water." Mizuno (1964) also began distinguishing mudflow deposits from debris-flow deposits, with the latter including those of an avalanche type. In field studies of volcanoes in Hokkaido and the Tohoku region of northern Honshu, he found many examples of distal volcaniclastic deposits of debris-flow origin containing "flow mounds." At Iwaki volcano (Mizuno 1975) described two mound-bearing debris-flow deposits, one of "flow type" and the other of "avalanche type," the latter not showing evidence of water involvement. Both are now classified as debris-avalanche deposits (Inokuchi 2006). Ando and Yamagishi (1975), during a study of deposits at Shikaribetsu volcano in Hokkaido, concluded that many of the "mudflow hills" at the base of Japanese volcanoes were formed by either hot or cold avalanches. Nakamura (1978) recognized that the 1888 Bandai deposit was not water-saturated and introduced the term "volcanic dry avalanche," terminology followed by Ui (1983) and Ui et al. (1986) in the first global and regional reviews of debris avalanches.

Work since 1980 has shown that the line between debris avalanches and lahars can be blurred. When sufficient water is available, avalanches can transform in part or entirely to lahars (Palmer et al., 1991), with the lahar facies of collapse events dominating. Partial transformation often occurs (e.g. Palmer et al. 1991; Zernack et al. 2009; Bernard et al. 2017; Bernard and Andrade 2019; Dufresne et al. 2020b -- this volume). Complete proximal transformation is common at smaller volume landslides such as those from Huila volcano in Colombia in 1994 (Scott et al. 2001; Worni et al. 2012) and Casita volcano in Nicaragua in 1998 (Scott et al. 2005) and has also been proposed for glaciated and hydrothermally altered Cascade Range (Vallance and Scott 1997; Scott et al. 2001) and Mexican stratovolcanoes (Carrasco-Núñez et al. 1993; Scott et al. 2001; Capra and Macias 2002; Capra et al. 2002), and elsewhere. Most lateral edifice-collapses behave as debris avalanches (Vallance and Iverson 2015), however, which can be locally saturated but retain characteristics of non-saturated flow throughout their extent (van Wyk de Vries et al. 2001; Siebert et al. 2004; Yoshida and Sugai 2010; Roverato et al. 2015).

4.2 Source Areas

As with debris-avalanche deposits themselves, interpretations of their source areas have varied widely. Originally attributed to tensional fissuring or erosion, they have often been viewed as either explosion craters and calderas or grabens and sector grabens formed by down-dropping of a segment of the edifice (Fernández Navarro 1924; Williams 1941; Williams and McBirney 1968; Macdonald 1972). Van Bemmelen (1949) referred to these features as volcano-tectonic rifts and distinguished those formed by slow lateral slipping of the cone and those formed by rapid landsliding or avalanching, in which case the sliding mass is fragmented. They have also been viewed as calderas or large maars (Waitz 1906) formed by explosive eruptions, as was postulated for Orotava valley in the Canary Islands (Rothpletz 1889; Wolf 1931; Hausen 1956) or caldera subsidence due to magma withdrawal accompanied by flank collapse and graben formation generating lahars as at Meru volcano (Cattermole 1982). Williams (1941) who introduced the term "explosion caldera," recognized that, for his two type examples, Bandai and Chaos Crags, avalanches rather than explosions were responsible for their large size. Ridley (1971) considered the massive collapse scarps on Tenerife, El Hierro and Lanzarote islands in the Canary Islands to be too large to have resulted from landslides and interpreted them as examples of trapdoor calderas, with collapse hinged at one end. Prior to the 1980 Mount St. Helens eruption Aramaki (1979) defined dry-avalanche deposits as formed by large-scale sector collapse of a volcanic cone, and Moriya (1980) used the term *horseshoe-shaped caldera* resulting from *Bandaian eruptions* in recognition of the relation between these features and the avalanche deposits below them.

Though the origin of volcanic debris avalanches is now understood, terminology for their source areas used after 1980 has been as varied as previous interpretations of their origin due to the ambiguity of many terms. They have often been referred to as calderas or craters, sometimes with morphological modifiers such as *horseshoe-shaped*, *U-shaped* or *breached*. Most avalanche source areas, however, are U-shaped rather than horseshoe-shaped, which is a common morphology of erosional depressions, and actual morphology can vary considerably. The 1980 collapse at Mount St. Helens has simply been referred to as a crater, although it and many others attain caldera-sized dimensions. Genetic modifiers such as *avalanche* have been used to distinguish these features from explosion calderas or erosion calderas, although *caldera* can have both genetic and morphological implications. The term *amphitheater* has often been used to avoid caldera comparisons, although in Roman usage, amphitheater refers to an enclosed, rather than open structure, the latter being referred to as a theater. The non-volcanic landslide community often uses the terms *scarp* or *scar*, either interchangeably or distinguishing a two-dimensional scarp (headwall and sidewall cliffs) from a scar, which includes the

floor of the failure zone as a third dimension. Bernard et al. (2020 - this volume) prefer use of the term *volcanic landslide scar* for these features.

4.3 Lateral Collapse Spectrum

In the years after the 1980 Mount St. Helens eruption lateral-collapse phenomena has been found to affect a wide spectrum of volcanic features in varying tectonic settings. This type of edifice failure is most common at steep-sided stratovolcanoes and lava dome complexes, but not all collapses of stratovolcanoes involve the central conduit and core of the volcano. Smaller flank collapses at stratovolcanoes are much more common, but some can be sizeable nonetheless, sometimes exceeding 0.1 km^3. On a much more massive scale, bathymetric studies have counter-intuitively demonstrated widespread occurrence of submarine VDADs originating from collapse of low-angle oceanic shield volcanoes as well as from post-eruption collapse of caldera walls or syn-eruptive collapse during caldera formation. Syn-eruptive large-scale collapse of stratovolcanoes has been documented during Pleistocene caldera formation in Kamchatka (Belousov et al. 2005), leaving stratovolcanoes with arcuate collapse scars perched on the rims of calderas. More recently Lavigne et al. (2013) have identified an estimated 2.1-2.9 km^3 of Rinjani volcano in Indonesia that collapsed into the newly forming Samalas caldera in 1257 AD. Collapse of walls of pre-existing calderas generating large-scale debris avalanches can occur during eruptions, as in 1988 when collapse of the east wall of Fernandina volcano in the Galapagos generated a 0.9 km^3 VDA that covered most of the caldera floor (Chadwick et al. 1991), or during non-eruptive periods long after the caldera-forming eruptions. Landslides on the scale of entire volcanic fields in the Absaroka Range near Yellowstone in Wyoming (Malone et al. 2017) and in the Markagunt Plateau of Utah (Hacker et al. 2014; Biek et al. 2019) rival the size of those from oceanic shield volcanoes. Fortunately, from a hazards perspective, frequency is inversely related to larger failure volume, and no VDADs of this size are known during the Holocene although conditions leading to collapse remain and future events cannot be ruled out.

5 Summary

Four decades later, the 1980 eruption of Mount St. Helens remains one of those seminal events that changed volcanologists' understanding of how volcanoes behave. The historical overviews in this paper selectively highlight the cumulative construction of volcanological concepts by those using (and adjusting) the building blocks available at the time. Examination of selected lateral-collapse events that produced debris-avalanche deposits volcanologists had worked on prior to 1980 illustrates the wide range of pre-St. Helens understanding of these events. These puzzling hummocky deposits clearly of volcanic materials but lying far beyond volcanoes were interpreted as a broad spectrum of both primary

and secondary volcanic or non-volcanic features. Contrary to general perception, however, the volcanological literature contained early accounts that recognized the landslide origin of some of these deposits. These remained hidden, almost in plain sight, mostly in regional and non-English publications that were not widely known. The burst of interest in volcano instability and lateral-collapse events after the 1980 eruption of Mount St. Helens has led to recognition of a thousand events from nearly 600 volcanoes. The last major volcaniclastic process to be widely recognized and understood, large-volume debris avalanches originating from lateral collapse of volcanic edifices have been found to be a relatively common occurrence in the life cycle of volcanoes across a wide spectrum of volcanic features and settings.

Acknowledgments

We acknowledge the incremental contributions of all those who led to the better understanding of volcano instability and related volcaniclastic processes both before and after the seminal events of May 18, 1980 at Mount St. Helens. The lengthy list of references below represents only a small fraction of those contributions. Reviews by Vince Neall and José-Luis Macías improved the manuscript.

References

Acosta J, Uchupi E, Muñoz A, Herranz P, Palomo C, Ballesteros M, ZEE Working Group (2004**)** Geologic evolution of the Canarian Islands of Lanzarote, Fuerteventura, Gran Canaria and La Gomera and comparison of landslides at these islands with those at Tenerife, La Palma and El Hierro. Mar Geophys Res 0:1-38

Adushkin VD, Gustintsev YA, Firstov PP (1984) On the origin of air waves during violent explosive eruptions Vulkanol-Seismol 5:3-11 (in Russian)

Alcaraz S (2002) Étude de l'avalanche de débris du Chimborazo, 35 000 BP (Équateur). Mém d'Aptitude Géol, IGAL Cergy-Pontoise, 266:104

Alloway B, McComb P, Neall V, Vucetich C, Gibb J, Sherburn S, Stirling M (2005) Stratigraphy, age, and correlation of voluminous debris-avalanche events from an ancestral Egmont volcano: Implications for coastal plain construction and regional hazard assessment. J R Soc N Z 35:229-267

Ando S, Yamagishi H (1975) Hill topography on the nuée ardente deposits of Shikaribetsu volcano, Hokkaido. Bull Volcanol Soc Jpn, 20:31-36 (in Jpn with Engl abstr)

Andrade SD (2009) The influence of active tectonics on the structural development and flank collapse of Ecuadorian ARC volcanoes. Diss, Univ Blaise Pascal-Clermont-Ferrand

Aramaki S (1979) Iwanami-shoten. Earth Sci 7:72, Tokyo

Barba D, Samaniego P, Eissen JP, Robin C, Fornari M, Cotten J, Beate B (2005) Geology and structure of the late Pleistocene to Holocene Chimborazo Stratovolcano (Ecuador). Int Symp Andean Geodyn Abstr Vol, Barcelona, España 90-93

Beate B, Hall ML (1989) Informe final de Volcanología: Tungurahua, Cotopaxi, Chimborazo. INECEL—Consultora San Francisco, Unpubl Rep, Parte C, 1-79

Beate B, von Hillebrandt C, Hall ML (1990) Mapa de los peligros volcánicos potenciales asociados con el volcán Chimborazo. Inst Geofís, Esc Politéc Nac, Quito

Begeat D (1900) Die aeolishen Inseln. Abhamdel K Akad D Wiss Math Phys Sci Cl 20:231

Begét JE and Kienle J (1992) Cyclic formation of debris avalanches at Mt. St. Augustine volcano, Alaska. Nature 356:701-704

Belousov AB (1995) The Shiveluch volcanic eruption of 12 November 1964— explosive eruption provoked by failure of the edifice. J Volcanol Geotherm Res 66:357-365

Belousov A, Belousova M (1996) Large scale landslides on active volcanoes in the 20th century - Examples from the Kurile-Kamchatka region (Russia). In: Senneset K (ed) Landslides. Balkema, Rotterdam

Belousov AB, Belousova MG (1998) Bezymyannyi eruption on March 30, 1956 (Kamchatka): Sequence of events and debris-avalanche deposits. Volcanol Seismol 20:29-47

Belousov A, Belousova M (2008) Large scale failures and debris avalanche deposits of volcanoes of Kurile Islands. Geophys Res Abstr 10:EGU2008-A-10672

Belousov A, Belousova M, Voight B (1999) Multiple edifice failures, debris avalanches and associated eruptions in the Holocene history of Shiveluch volcano, Kamchatka, Russia. Bull Volcanol 61:324–342

Belousov AB, Walter TR, Troll VR (2005) Large-scale failures on domes and Stratovolcanos situated on caldera ring faults: Sand-box modelling of natural examples from Kamchatka, Russia. Bull Volcanol 67(5):457-468

Belousov A, Voight B, Belousova M (2007) Directed blasts and blast-generated pyroclastic density currents: a comparison of the Bezymianny 1956, Mount St Helens 1980, and Soufrière Hills, Montserrat 1997 eruptions and deposits. Bull Volcanol 69:701–740

Belousova M, Belousov A (1995) Prehistoric and 1933 debris avalanches and associated eruptions of Harimkotan Volcano (Kurile Islands). Per Mineral (LXIV):99-101

Belousova M, Belousov A (2011) Tsunamigenic volcanic landslides of Kurile-Kamchatka arc. Geophys Res Abs 13:2011 EGU Gen Assemb

Bemmelen RW van (1949) The geology of Indonesia. Government Printing Office, The Hague

Bemmelen RW van (1954) Mountain Building. Martius Nijhoff, Hague, p 99-103

Bernard B (2008) Étude des dépôts d'avalanche de débris volcaniques: analyse sédimentologique d'exemples naturels et identification des mécanismes de mise en place. Diss, Univ Blaise Pascal-Clermont-Ferrand

Bernard B, Andrade SD (2019) Large volcanic debris avalanches in Ecuador. Abstract vol 8th Int Symp Andean Geodyn, Quito, Ecuador, 24-26 September 2019

Bernard B, van Wyk de Vries B, Barba B, Robin C, Leyrit H, Alcaraz S, Samaniego P (2008). The Chimborazo sector collapse and debris avalanche: deposit characteristics as evidence of emplacement mechanisms. J Volcanol Geotherm Res 176:36-43

Bernard B, Takarada S, Andrade D, Dufresne A (2020) Terminology and strategy to describe volcanic landslides and debris avalanches. In: Roverato M, Dufresne A, Procter JN (eds) Volcanic Debris Avalanches: From Collapse to Hazard. Springer Book Series Advances in Volcanology, this volume

Benitez Padilla S (1946) Síntesis geológica del Archipelago Canario. Estud Geol (Madrid) 3:3-19

Biek RF, Rowley PD, Hacker DB (2019) The gigantic Markagunt and Sevier gravity slides resulting from mid-Cenozoic catastrophic mega-scale failure of the Marysvale volcanic field, Utah, USA. Geol Soc Am Field Guide 56:1-121

Black PM (1970) Observations on White Island Volcano. N Z Bull Volcanol 34(1):158–167

Blahůt J, Balek J, Klimeš J, Rowberry M, Kusák M, Kalina J (2019) A comprehensive global database of giant landslides on volcanic islands. Landslides https://doi.org/10.1007/s10346-019-01275-8

Bogoyavlenskaya GE, Braitseva OA, Melekestsev IV, Kiriyanov VY, Miller CD (1985) Catastrophic eruptions of the directed-blast type at Mount St. Helens, Bezymianny and Shiveluch volcanoes. J Geodyn 3:189-218

Bossard L (1928) Origin of the conical hills in the neighbourhood of Mount Egmont. N Z J Sci Technol 10:119-25

Boudon G, Le Friant A, Komorowski JC, Deplus C, Semet MP (2007) Volcano flank instability in the Lesser Antilles Arc: diversity of scale, processes, and temporal recurrence. J Geophys Res, Solid Earth 112(B8)

Bravo T (1962) El circo de Las Cañadas y sus dependencias: Bol R Soc Esp Hist Nat 60:93-108

Bronto S (1989) Volcanic geology of Galunggung, West Java, Indonesia. Diss Univ Canterbury, N Z

Bruggen J (1942) Geologia de la puna de San Pedro de Atacama y sus formaciones de areniscas y arcillas rojas. An primer Congr Panam Ing Minas Geol, Tomo 1:374

Buch L von (1825) Physikalische Beschreibung der Kanarischen Inseln. vol. 2 Hofdruckerei von Königlichen Akademie, Berlín

Bullard FM (1976) Volcanoes of the Earth. Austin, Univ Texas Press, 579 p

Camus G, Diament M**,** Gloaguen M, Provost A, Vincent PM (1992) Emplacement of a debris avalanche during the 1883 eruption of Krakatau (Sunda Straits, Indonesia). Geojoumal 28(2):123-128

1109 Capra L, Macias JL (2002) The cohesive Naranjo debris-flow deposit: a dam breakout flow derived
1110 from the Pleistocene debris-avalanche deposit of Nevado de Colima Volcano (Mexico). J
1111 Volcanol Geotherm Res 117:213-235

1112 Capra L, Macías JL, Scott KM, Abrams M, Garduño-Monroy (2002) Debris avalanches and debris
1113 flows transformed from collapses in the Trans-Mexican Volcanic Belt, Mexico -- behavior, and
1114 implications for hazard assessment. J Volcanol Geotherm Res 113:81-110
1115
1116 Carrasco-Núñez G, Vallance JW, Rose WI (1993) A voluminous avalanche-induced lahar from
1117 Citlaltèpetl volcano, Mexico: Implications for hazard assessment. J Volcanol Geotherm Res
1118 59:35-46
1119
1120 Cattermole P (1982) Meru—A Rift Valley giant. Volcano News 11:1–3

1121 Chadwick WW Jr, De Roy T, Carrasco A (1991) The September 1988 intracaldera avalanche and
1122 eruption at Fernandina volcano, Galapagos Islands. B Volcanol 53(4):276-286

1123 Chiba S, Kimura J-I (2001) Geology and growth history of Bandai volcano, Tohoku-Honshu arc,
1124 Japan – Analysis of volcanic activity by tephrochronology. Jpn Mag Mineral Petrol
1125 Sci 30:126– 156 (in Jpn with Engl abstr)

1126 Christiansen RL (1982) Volcanic hazard potential in the California Cascades. In: Martin RJ and
1127 Davis JF (eds) Status of volcanic prediction and emergency response capabilities in volcanic
1128 hazard zones of California. Calif Div Mines Geol Spec Publ 63:II-43 - II-65

1129 Clapperton C (1983) The glaciation of the Andes. Quat Sci Rev 2:83-155

1130 Clapperton MC (1990) Glacial and volcanic geomorphology of the Chimborazo–Carihuairazo
1131 Massif, Ecuadorian Andes. Trans R Soc Edinburgh, Earth Sci 81:91-116

1132 Clark RH, Cole JW (1986) White Island. In: Smith IEM (Ed.), Late Cenozoic Volcanism in New
1133 Zealand. R Soc N Z Bull 23:169-178

1134 Clouard V, Bonneville A (2004) Submarine Landslides in French Polynesia. In: Hekinian R,
1135 Cheminée JL, Stoffers P (eds) Oceanic Hotspots. Springer, Berlin, Heidelberg
1136

1137 Coello, J (1973) Las series volcánicas en subsuelos de Tenerife. Estud Geol Madrid 29:491-512

1138 Cole JW (1986) Monitoring White Island Volcano. In: Gregory JG, Watters WA (eds), Volcanic
1139 Hazards Assessment in New Zealand. N Z Geol Surv Record 10:55-59

1140 Cole JW, Thordarson T, Burt RM (2000) Magma origin and evolution of White Island (Whakaari)
1141 volcano, Bay of Plenty, New Zealand. J Petrol 41:867-895

1142 Cooke RJS (1981) Eruptive history of the volcano Ritter Island. In: Johnson RW (ed) Cooke-Ravian
1143 volume of volcanological papers. Geol Surv Papua New Guin Mem 10:115-123

1144 Coombs ML, White SM, Scholl DW (2007) Massive edifice failure at Aleutian arc volcanoes. Earth
1145 Planet Sci Lett 256:403–418
1146
1147 Cortes A, Garduno VH, Navarro C, Komorowski JC, Saucedo R, Macias JL, Gavilanes JC (2005)
1148 Carta Geológica del Complejo Volcánico de Colima, Con Geología del Complejo Volcánico de
1149 Colima. Cartas Geol Mineras, Univ Nac Auton Mex 10

1150 Cortes A, Macías JL, Capra LL, Garduño-Monroy VH (2010) Sector collapse of the SW flank of
1151 Volcán de Colima, México. The 3600 yr BP La Lumbre-Los Ganchos debris avalanche and
1152 associated debris flows. J Volcanol Geotherm Res 189(1-4):52-66

1153 Cortes A, Komorowski J-C, Macías JL, Capra L, Layer PW (2019) Late Pleistocene-Holocene
1154 debris avalanche deposits from Volcán de Colima, México. In: Varley N, Conner CB,
1155 Komorowski J-C (eds) Volcán de Colima Portrait of a Persistantly Hazardous Volcano. Berlin:
1156 Springer, p 55-80

1157 Cotton CA (1944) Volcanoes as Landscape Forms. Whitcombe & Tombs Ltd., Christchurch, N Z

1158 Crandell D (1989) Gigantic debris avalanche of Pleistocene age from ancestral Mount Shasta
1159 Volcano, California, and debris avalanche hazard zonation. US Geol Surv Bull 1861:1–32
1160
1161 Crandell DR, Mullineaux DR, Sigafoos RS, Rubin M (1974) Chaos Crags eruptions and rockfall-
1162 avalanches, Lassen Volcanic National Park, California. J Res U S Geol Surv 2(1):49-59

1163 Crandell D, Miller C, Glicken H, Christiansen R, Newhall C (1984) Catastrophic debris avalanche
1164 from ancestral Mount Shasta Volcano, California. Geology 12:143-146

1165 Cronin SJ, Ferland MA, Terry JP (2004) Nabukelevu volcano (Mt. Washington), Kadavu–a source
1166 of hitherto unknown volcanic hazard in Fiji. J Volcanol Geotherm Res 131:371-396

1167 Cronin SJ, Neal VE (1997). A late Quaternary stratigraphic framework for the northeastern
1168 Ruapehu and eastern Tongariro ring plains, New Zealand. N Z J Geol Geophys 40:185-197

1169 Dall WH (1884) A new volcano island in Alaska. Science 3(51):89-93

1170 Davidson G (1884) Notes on the eruption of Mount St. Augustine, Alaska, October 6, 1883.
1171 Science 3(54):186-189

1172 Davies T, McSaveney M, Kelfoun K (2010) Runout of the Socompa volcanic debris avalanche,
1173 Chile: a mechanical explanation for low basal shear strength. Bull Volcanol 72:933-944

1174 Day S, Llanes P, Silver E, Hoffmann G, Ward S, Driscoll N (2015) Submarine landslide deposits of
1175 the historical lateral collapse of Ritter Island, Papua New Guinea. Mar Petrol Geol 67:419-438
1176
1177 Delcamp A, Delvaux D, Kwelwa S, Macheyeki A, Kervyn M (2016) Sector collapse events at
1178 volcanoes in the north Tanzanian divergence zone and their implications for regional tectonics.
1179 Geol Soc Am 128:169–186
1180
1181 Delcamp A, Kervyn M, Benbakkar M, Kwelwa S, Peter D (2017) Large volcanic landslide and
1182 debris avalanche deposit at Meru, Tanzania. Landslides 14:833–847 DOI 10.1007/s10346-016-
1183 0757-8
1184
1185 Demant A (1979) Volcanología y petrografía del sector occidental del eje neovolcánico. Univ Nac
1186 Autón Méx Inst Geol Revista 3(1):39-57

1187 Denlinger RP, Morgan JK (2014) Instability of Hawaiian volcanoes. In: Poland MP, Takahashi JP,
1188 Landowski CM (eds) Characteristics of Hawaiian volcanoes. U S Geol Surv Prof Pap 1801:149-176

Deplus C, Bonvalot S, Dahrin D, Diament M, Harjono H, Dubois J (1995) Inner structure of the Krakatau volcanic complex (Indonesia) from gravity and bathymetry data. J Volcanol Geotherm Res 64:23-52

Deplus C, Le Friant A, Boudon G, Komorowski .C, Villemant B, Harford C, Ségoufin J, Cheminée JL (2001) Submarine evidence for large-scale debris avalanches in the Lesser Antilles Arc. Earth Planet Sci Lett 192:145–157

Detterman RL (1973) Geologic map of the Iliamna BB2 quadrangle, Augustine Island, Alaska. U S Geol Surv Geol Quad Map GQ-1068, scale 1:63,500

Deruelle B (1978) The Negras de Aras nuée ardente deposits: a cataclysmic eruption of Socompa volcano (Andes of Atacama, north Chile). Bull Volcanol 413:175-186

Deruelle B, Brousse R (1984) "Nuee ardente" deposits at Tata Sabaya volcano (Bolivian-Chilean Andes): pumices and lava blocks crystallised from a single magma at different depths. Rev Geol Chile 22:3-15

De Silva SL., Davidson JP, Croudace IW, Escobar A (1993) Volcanological and petrological evolution of Volcan Tata Sabaya, SW Bolivia. J Volcanol Geotherm Res 55:305-335

Detterman RL (1973) Geologic map of the Iliamna BB2 quadrangle, Augustine Island, Alaska. U S Geol Surv Geol Quad Map GQ-1068, 1:63,360 scale

Diller JS et al (1915) Guidebook of the western United States, Part D, The Shasta route and coastline: U S Geol Surv Bull 614:1-146

Downie C, Wilkinson (1972) The geology of Kilimanjaro. Dept Geol Sheffield Univ, 253 p

Dufresne A, Siebert L, Bernard B, Sparks RSJ, Takarada S, Clavero J, Belousov A, Belousova M (2008) Volcanic debris avalanche deposit database—a progress report. IAVCEI Gen Assemb, Iceland

Dufresne A, Siebert L, Bernard B (2020a) Distribution and geometric parameters of volcanic debris avalanche deposits. In: Roverato M, Dufresne A, Proctor JN (eds) Volcanic Debris Avalanches: From Collapse to Hazard. Springer Book Series Advances in Volcanology, this volume)

Dufresne A, Zernack AV, Bernard K, Thouret J-C, Roverato M (2020b) Sedimentology of volcanic debris avalanche deposits. In: Roverato M, Dufresne A, Procter JN (ed) Volcanic Debris Avalanches: From Collapse to Hazard. Springer Book Series Advances in Volcanology, this volume

Duncan AR (1970). The petrology and petrochemistry of andesite volcanoes in Eastern Bay of Plenty, New Zealand. PhD Thesis, Victoria Univ Wellington, N Z

Eakins B, Robinson JE, Kanamatsu T, Naka J, Smith JR, Takahashi E, Clague DA (2004) Hawaii's Volcanoes Revealed. U S Geol Surv Invest Ser I-2809

Escher BG (1925) L'eboulement prehistorique de Tasikmalaja et le Volcan Galunggung. Leidische Geol Medeelingen 1(1):8-21

Eppler DB, Fink J, Fletcher R (1987) Rheological properties of the Chaos Jumbles rock fall avalanche, Lassen Volcanic National Park, California. J Geophys Res 92:3623–3633

1230 Fenner CN (1923) The origin and mode of emplacement of the great tuff deposit in the Valley of
1231 Ten Thousand Smokes. Natl Geog Soc Contr Tech Pap, Katmai Ser no 1:1-74

1232 Fernández Navarro L (1924) Estudios hydrogeológicos en al Valle de la Orotava. Imprenta A
1233 Romero, Santa Cruz de Tenerife, 95 pp

1234 Francis P (1976) Volcanoes. Penguin Books, Harmondsworth, Middlesex, England, 368 pp

1235 Francis PW, Ramirez CF (1985) "Nuée ardente" deposits at Tata Sabaya volcano: a re-
1236 interpretation. Rev Geol Chile 24:107-110

1237 Francis PW, Wells GL (1988) Landsat Thematic Mapper observation of debris avalanche deposits
1238 in the Central Andes. Bull Volcanol 50:258-278

1239 Francis PW, Roobol MJ, Walker GPL (1974) The San Pedro and San Pablo volcanoes of north
1240 Chile and their hot avalanche deposits. Geol Rundsch 63:357-388

1241 Francis PW, Gardeweg M, Ramirez CF (1985) Cataclastic debris avalanche deposits of the
1242 Socompa volcano, northern Chile. Geology 13:600-603

1243 Fritsch K, Reiss W (1868) Geologische Beschreibung der Insel Tenerife. Wurster. Winterthur, 496
1244 p

1245 Furuya T (1974) A geomorphological consideration of the Mayu-yama great landslide in 1792.
1246 Disaster Prev Res Inst Annu, Kyoto Univ 17B:259-264

1247 Furuya T (1978) Preliminary report on some volcanic disasters in Indonesia. South East Asian Stud
1248 15(4):591-597

1249 Fuster JM, Araña V, Brandle JL, Navarro M, Alonso U, Aparicio A (1968) Geología y volcanología
1250 de las islas Canarias. Madrid, Tenerife Instituto 'Lucas Mallada', CSIC
1251
1252 Gaylord DR, Neall VE, Palmer AS (2014) The Middle Pleistocene Maitahi Formation, Taranaki,
1253 New Zealand: a new formal lithostratigraphic unit. N Z J Geol Geophys 57(4):369-377 DOI:
1254 10.1080/00288306.2014.914041
1255
1256 Ghiglieri G, Pittalis D, Cerri G, Oggiano G (2012) Hydrogeology and hydrogeochemistry of an
1257 alkaline volcanic area: The NE Mt. Meru slope (East African Rift, northern Tanzania). Hydrol
1258 Earth Syst Sci 16:529–541 doi: 10 .5194 /hess -16 -529-2012
1259
1260 Girina OA (2013) Chronology of Bezymianny Volcano activity, 1956-2010. J Volcanol Geotherm
1261 Res 263:22-41
1262
1263 Glicken H (1996) Rockslide-Debris Avalanche of May 18, 1980, Mount St. Helens Volcano,
1264 Washington. U S Geol Surv Open-file Rep 96-677:1-90 and 5 plates
1265

1266 Glicken H, Asmoro P, Lubia H, Frank D, Casadevall TC (1987) The 1772 debris avalanche and
1267 eruption at Papandayan volcano, Indonesia, and hazards from future similar events. Hawaii
1268 Symp on How Volcanoes Work (abstr) U S Geol Surv Hawaii Volc Observ

1269 Godoy B, Clavero J, Rojas C, Godoy E (2012) Facies volcánicas del depósito de avalancha de
1270 detritus del volcán Tata Sabaya, Andes Centrales. Andean Geol 39(3):394-406
1271

Gorshkov GS (1959) Gigantic eruption of the volcano Bezymianny. Bull Volcanol 20:77-109

Gorshkov GS (1963) Directed volcanic blasts. Bull Volcanol 26:83-88

Gorshkov GS (1970) Volcanism of the Upper Mantle: Investigations in the Kuril Island Arc. Plenum Press, N Y

Gorshkov GS, Bogoyavlenskaya GE (1965) Bezymianny volcano and peculiarities of its last eruption (1955–1963). Moscow, Nauka (in Russian)

Gorshkov GS, Dubik YM (1970) Gigantic directed blast at Shiveluch volcano (Kamchatka). Bull Volcanol 34:262-288

Grange LI (1931) Conical hills on Egmont and Ruapehu volcanoes. N Z J Sci Tech 12:376-84

Griggs RF (1920) The great Mageik landslide. Ohio J Sci 20:325-354

Griggs RF (1922) The Valley of Ten Thousand Smokes. Nat Geog Soc 1:340

Grilli ST, Tappin DR, Carey S, Watt SFL, Ward SN, Grilli AR, Engwell SL, Zhang C, Kirby JT, Schambach L, Muin M (2019) Modelling of the tsunami from the December 22, 2018 lateral collapse of Anak Krakatau volcano in the Sunda Straits, Indonesia. Sci Rep 9:11946

Hacker DB, Biek RF, Rowley PD (2014) Catastrophic emplacement of the gigantic Markagunt gravity slide, southwest Utah—implications for hazards associated with sector collapse of volcanic fields. Geology 42(11):943-946

Hackett WR, Houghton BF (1986) Active composite volcanoes of Taupo volcanic zone. Central North Island Volcanism, Int Volcanol Cong Tour Guides: Day One, White Island. N Z Geol Surv, Lower Hutt 21:65-72

Hamilton EL (1957) Marine geology of the southern Hawaiian Ridge. Bull Geol Soc Am 68:1011-1026

Hamilton WM, Baumgart IL (1959) White Island. N Z Sci Indus Res Bull 127:1-84

Hammer KL (1907) Die geographische Verbreitung der vul kanischen Gebilde und Erscheinungen im Bismarck archipel und auf den Salomonen. Diss Ludwigs Univ

Hashimoto N, Kawano T, Isoyama K, Kuboki J, Okumi S (1976) A geomorphological study of the Nirasaki pyroclastic flow and its mud-flow hills, Yamanashi Prefecture. Bull Geol Surv Jpn 27(9):625-633 (in Jpn with Engl abs)

Hausen H (1956) Contributions to the geology of Tenerife. Soc Sci Fenn Comm Phys-Math 18:1-247

Hausen H (1969) Some contributions to the geology of La Palma. Soc Sci Fenn, Comment Phys-Math 35:1-140

Hausen H (1970) Desprendimientos en las Islas Canarias. Anu Estud Atl 16:531-559

Hausen H (1973) Outlines of the geology of Hierro (Canary Islands. Soc Sci Fenn, Comment Phys-Math 43:65-148

Heath J P (1960) Repeated avalanches at Chaos Jumbles, Lassen Volcanic National Park. Am J Sci 258:744-751

Herrick JA, Siebert L, Rose WI (2013) Large-volume Barriles and Caisán debris avalanche deposits from Volcán Baru, Panama. In: Rose,WI, Palma JL, Delgado Granados H, Varley N (eds) Understanding Open-Vent Volcanism and Related Hazards. Geol Soc Am Spec Pap 498:1–22

Hildreth W, Fierstein J, Lanphere MA, Siems DF (2000) Mount Mageik: A compound stratovolcano in Katmai National Park. In: Kelley KD, Gough LP (eds) Geologic Studies in Alaska by the U.S. Geological Survey, 1998, U S Geol Surv Prof Pap 1615:23-41

Hill H (1905) Taupo Plateau and Lake: a retrospect and prospect. Trans NZ Inst, Hamilton A (ed) 37:445-464

Hodgson KA (1993) Late Quaternary lahars from Mount Ruapehu in the Whangaehu River valley, North Island, New Zealand. PhD thesis, Massey Univ, Palmerston North, 2 vol., 256 and 112 pp, maps

Holcomb RT, Searle RC (1991) Large landslides from oceanic volcanoes. Mar Geotechnol 10:19-32

Horsfield Th (1816) On the mineralogy of Java. Verh Bataviaasch Genoot Kunsten Wet, 8:141-173

Hoshizumi H, Uto K, Watanabe K (1999) Geology and eruptive history of Unzen volcano, Shimabara Peninsula, Kyushu, SW Japan. J Volcanol Geotherm Res 89:81-94

Hotz PE (1977) Geology of the Yreka quadrangle, Siskiyou County, California. U S Geol Surv Bull 1436:1-72

Hoyt DV (1978) An explosive volcanic eruption in the Southern Hemisphere in 1928. Nature 275:630-632

Hubp JL, Martín del Pozzo AL, Vázquez-Selem L (1993) Estudio geomorfológico del complejo volcánico de Colima. Geofís Int 32 (4):633-641

Hunt JE, Talling PJ, Clare MA, Jarvis I, Wynn RB (2014) Long-term (17 Ma) turbidite record of the timing and frequency of large flank collapses of the Canary Islands. Geochem Geophys Geosyst 15:3322-3345, doi:10.1002/2014GC005232

INEGI (1984) Carta Geológica (Geological map). 1:50000. Inst Nac Estat, Geogr Inform, Hojas EI3B35, EI3B34. Ciudad de Méx

Inokuchi T (1988) Gigantic landslides and debris avalanches on volcanoes in Japan: Case studies on Bandai, Chokai, and Iwate Volcanoes. Rep Nat Res Center Disaster Prev 41:163-275 (in Jpn with Engl abstr)

Inokuchi T (2006) Properties of sector-collapse and debris avalanche on Quaternary volcanoes in Japan. J Jpn Landslide Soc 42(5):409-420 (in Jpn)

Jacobs TJ (1844) Scenes, Incidents and Adventures in the Pacific Ocean, or the Islands of the Australasian Seas, During the Cruise of the Clipper Margaret Oakley Under Capt. Benjamin Morell. Harper & Bros, New York

Jaggar TA (1930) Some analogous bowlder hillocks. Volc Lett 286:3

Johnson RW (1987) Large-scale volcanic cone collapse: the 1888 slope failure of Ritter volcano, and other examples from Papua New Guinea. Bull Volcanol 49:669–679

Johnson RW (2013) Fire Mountains of the Islands: A History of Volcanic Eruptions and Disaster Management in Papua New Guinea and the Solomon Islands, ANU Press, Acton, Australia

Judd JW (1903) Volcanoes: what they are and what they teach. D. Appleton, New York, 381 pp

Junghuhn F (1853) Java, its shape, covering, and internal structure. 2nd ed, Part 2, Amsterdam

Juwarna H, Wirakusumah AD, Soetoyo, Bronto S (1986) Geologic map of Galunggung volcano, West Java. Volc Surv Indon

Karstens J, Berndt C, Urlaub M, Watt SFL, Micallef A, Ray M, Klaucke I, Muff S, Klaeschen D, Kühn M, Roth T, Böttner C, Schramm B, Elger J, Brune S (2019) From gradual spreading to catastrophic collapse – reconstruction of the 1888 Ritter Island volcanic sector collapse from high-resolution 3D seismic data. Earth Planet Sci Lett 517:1–13

Katayama N (1974) Old records of natural phenomena concerning the "Shimabara Catastrophe." Sci Rep Shimabara Volcano Obs, Kyushu Univ, Faculty Sci 9:1-45 (in Jpn with Engl abstr)

Katili JA, Sudradjat A (1984) Galunggung. The 1982-1983 Eruption. Volcanol Surv Indon, 102 p

Kelfoun K, Druitt TH (2005) Numerical modelling of the Socompa rock avalanche, Chile. J Geophys Res 110:B12202

Kelfoun K, Druitt TH, van Wyk de Vries B, Guilbaud M-N (2008) Topographic reflection of the Socompa debris avalanche, Chile. Bull Volcanol 70(10):1169-1187

Kemmerling GLL (1921) De geologie en geomorfologie van den Idjen. Het Idjen Hoogland. - Uitg Kon Natuurk. Ver, Batavia

Kienle J, Forbes RB (1976) Augustine—evolution of a volcano. Geophys Inst Annu Rep 1975–1976:26-48

Kienle J, Swanson SE (1980) Volcanic hazards from future eruptions of Augustine Volcano, Alaska. Fairbanks, Univ Alaska Geophys Inst, document R-275:1-126 and map

Kienle J, Swanson SE (1983) The hazards of Augustine. Northern Eng 15(3):10-37

Kilian R (1987) The development of the Chimborazo (6310 m), Carihuairazo (5106 m) and other volcanoes of Ecuador. Zbl Geol Paläont Teil I, Stuttgart 955-965

Kilian R, Hegner E, Fortier S, Satir M (1995) Magma evolution within the accretionary mafic basement of Quaternary Chimborazo and associated volcanoes (Western Ecuador). Rev Geol Chile 22:203-218

Komorowski JC, Navarro C, Cortes A, Saucedo R, Gavilanes JC, Siebe C, Espindola JM, Rodriguez-Elizarraras SR (1997) The Colima Volcanic Complex. Field guide 3. IAVCEI, Gen Assemb, Puerto Vallarta

Koto B (1916) On the volcanoes of Japan, III. J Geol Soc Jpn 23:29-55

Krastel S, Schmincke H-U, Jacobs CL, Rihm R, Le Bas TP, Alibés B (2001) Submarine landslides around the Canary Islands, J Geophys Res 106(B3), 3977-3997

Lamb HH (1970) Volcanic dust in the atmosphere; with a chronology and assessment of its meterological significance. Philos Trans R Soc Lond A266:425-533

Langford SA, Brill RC (1972) Giant submarine landslides on the Hawaiian Ridge: A rebuttal. Pac Sci 26:254-258

Latter JH (1981) Tsunamis of volcanic origin: summary of causes, with particular reference to Krakatoa, 1883. Bull Volcanol 44(3):467-490

Lavigne F, Degeai J-P, Komorowski J-C, Guillet S, Robert V, Lahitte P, Oppenheimer C, Stoffel M, Vidal CM, Surono, Pratomo I, Wassmer P, Hajdas I, Danang Sri Hadmoko DS, de Belizal E (2013) Source of the great A.D. 1257 mystery eruption unveiled, Samalas volcano, Rinjani Volcanic Complex, Indonesia. Proc Nat Acad Sci 110(42):16,742-16,747

Luhr JF, Carmichael ISE (1980) The Colima Volcanic Complex: I. Post-caldera andesites from Volcán Colima. Contrib Mineral Petrol 71:343-372

Luhr JF, Carmichael ISE (1982) The Colima Volcanic Complex: III. Ash- and scoria-fall deposits from the upper slopes of Volcán de Colima. Contrib Mineral Petrol 80:262-275

Luhr JF, Prestegaard KL (1988) Caldera formation at Volcán Colima, Mexico, by a large Holocene volcanic debris avalanche. J Volcanol Geotherm Res 35:335-348

Lukmantara L (1983) Genesis gumuk piroklastika dataran Jember, Jawa Timur. Skripsi Sarjana, UNPAD, Bandung

Macdonald GA (1972) Volcanoes. Prentice-Hall, Englewood Cliffs, NJ

Macdonald GA, Abbott AT (1970) Volcanoes in the Sea: The Geology of Hawaii. Univ Press Hawaii, Honolulu, 441 pp

Mack S (1960) Geology and ground-water resources of Shasta Valley, Siskiyou County, California: U S Geol Surv Water-Supply Pap 1484:1-115

MacLeod N (1989) Sector-failure eruptions in Indonesia volcanoes. Geol Indon 12:563-601

Malloy L (1998) Soils in the New Zealand Landscape – the Living Mantle, 2nd Ed. N Z Soc Soil Sci

Malone DH, Craddock JP, Schmitz MD, Kenderes S, Kraushaar B, Murphey CJ, Nielsen S, Mitchell TM (2017) Volcanic initiation of the Eocene Heart Mountain Slide, Wyoming, USA. J Geol 125(4):439-457

Martí J (2019) Las Cañadas caldera, Tenerife, Canary Islands: A review, or the end of a long volcanological controversy. Earth Sci Rev 196:102889

1439 Mason AC, Foster HL (1956) Extruded mudflow hills of Nirasaki, Japan. J Geol 64:74-83
1440
1441 Masson DG, Watts AB, Gee MJR, Urgeles R, Mitchell NC, Le Bas TP, M Canals M (2002) Slope
1442 failures on the flanks of the western Canary Islands. Earth Sci Rev 57(1–2):1-35
1443 McMurtry GM, Watts P, Fryer GJ, Smith JR, Imamura F (2004) Giant landslides, mega-tsunamis,
1444 and paleo-sea level in the Hawaiian Islands. Mar Geol 203:219-233
1445 Melekestsev IV, Braitseva OA (1988) Giant collapses on volcanoes. Volcanol Seismol 6:495-508
1446 Mimura K, Kawachi S, Fujimoto U, Taneichi M, Hyuga T, Ichikawa S, Koizumi M (1982) Debris
1447 avalanche hills and their natural remnant magnetization: Nirasaki debris avalanche, central
1448 Japan. J Geol Soc Jpn 88:653-663 (in Jpn with Engl abstr)
1449
1450 Misawa, K (1924) Small mounds at the south-western foot of volcano Yatsuga-dake: Chiri Kyoiku
1451 (Geog Education) 1(2)
1452 Mitchell NC (2003) Susceptibility of mid-ocean ridge volcanic islands and seamounts to large-scale
1453 landsliding. J Geophys Res 108(B8): 2397, doi:10.1029/2002JB001997
1454 Miyatake K (1934) On the explosion of volcano Harumukotan-jima, Central Kurile (Chishima), in
1455 Jan. 1933. Bull Volcanol Soc Jpn 2:76-85 (in Jpn)
1456 Mizuno Y (1964) Landforms associated with volcanic debris flows at the foot of Zao volcano.
1457 Hirosaki Univ Fac Educ Bull 13:23-32 (in Jpn)
1458 Mizuno Y (1975) Piedmont geomorphology of Iwaki volcano. Tohoku Univ Sci Rep Ser 7 25:159-
1459 164
1460 Mohr JM (1773) Verh Holl Mij Wetench, part 14
1461 Moon V, Bradshaw J, de Lange W (2009) Geomorphic development of White Island Volcano
1462 based on slope stability modelling. Eng Geol 104:16-30
1463 Moore JG (1964) Giant submarine landslides on the Hawaiian Ridge. U S Geol Surv Prof Paper
1464 501-D:95-98.
1465 Moore JG, Clague DA, Holcomb RT, Lipman PW, Normark WR, Torresan M (1989) Prodigious
1466 submarine landslides on the Hawaiian Ridge. J Geophys Res 94:17465-17484
1467
1468 Moore JG, Normark WR, Holcomb RT (1994) Giant Hawaiian landslides. Annu Rev Earth Planet
1469 Sci 22:119-144
1470
1471 Mooser F (1961) Los volcanes de Colima. Univ Nal Auton Mex Inst Geol Bol 61:49-71
1472 Montanaro C, Beget J (2011) Volcano collapse along the Aleutian Ridge (western Aleutian Arc).
1473 Nat Hazards Earth Syst Sci, 11:715–730
1474 Morgan JK, Silver E, Camerlenghi A, Dugan B, Kirby S, Shipp C, Suyehiro K (2009) Addressing
1475 geohazards through ocean drilling. Sci Drill no 7:15-30
1476 Morgan PO, Gibson W (1927) The geology of Egmont Subdivision. N.Z. Geol Surv Bull 29:1-99

Moriya I (1980) "Bandaian Eruption" and landforms associated with it. Collection of articles in memory of retirement of Prof. K. Nishimura from Tohoku Univ, p 214-219 (in Jpn with Engl abstr)

Mulyana AR, Sumpena AD, Pujowarsito, Ridwan I, Rukada T (2007) Volcanic hazard map of Raung volcano, East Java Province. Cent Volcanol Geol Hazard Mitig, 1:100,000 scale

Murai I (1961) A study of the textural characteristics of pyroclastic flow deposits in Japan. Bull Earthq Res Inst Tokyo Univ 39:133-248

Nakamura Y (1978) Geology and petrology of Bandai and Nekoma volcanoes. Tohoku Univ Sci Rep, ser 3, 14:67-119

Neall VE (1979) Sheets P19, P20 and P21, New Plymouth, Egmont and Manaia: Geological Map of New Zealand: Wellington, N Z Dept Sci Ind Res, scale 1:50,000, 3 maps and notes, 36

Neall VE (2002) Review of flank collapse at New Zealand volcanoes. Montagne Pelee 1902-2002 Explosive volcanism in subduction zones, St. Pierre, Martinique, May 12-16, 2002 Abstr p 71

Neall VE, Stewart RB, Smith IEM (1986) History and petrology of the Taranaki volcanoes. R Soc N Z Bull 23:251-263

Neumann van Padang M (1929) De noordelijke doorbraak in den Papandajan kraterwand. Mijningenieur 10:52-58, map

Neumann van Padang M (1939) Über die vielen tausend Hügel in westlichen Vorlande des Raoeng-Vulkans (Ostjava). Ingenieur Nederlandsch-Indie 6(4):35-41

Newhall CG, Self S (1982) The Volcanic Explosivity Index (VEI): An estimate of explosive magnitude for historical volcanism. J Geophys Res 87(C2):1231-1238

Nozaki T (2015) Historical and pre-historical gigantic landslides in Tateyama Caldera and their mechanism of occurrence. 10th Asian Reg Conf Int Assoc Eng Geol

O'Callaghan and Francis PW (1986) Volcanological and petrological evolution of San Pedro volcano, Provincia El Loa, North Chile. J Geol Soc Lond 143:275-286

Ogawa T (1932) Pleistocene glaciation in central Japan. Chikyu (The Globe) 17(3):1-12

Ota K (1969) Study on the collapses in the Mayu-yama—1. On the mechanism of collapse. Rep Shimabara Inst Volcanol Balneol Fac Sci Kyushu Univ 5:6-35

Paguican C, Roverato M, Yoshida H (2020) Volcanic debris avalanche transport and emplacement mechanisms In: Roverato M, Dufresne A, Proctor JN (eds) Volcanic Debris Avalanches: From Collapse to Hazard. Springer Book Series Advances in Volcanology, this volume)

Palacios D (1994) The origin of certain wide valleys in the Canary Islands. Geomorphology 9:1-18

Palmer BA, Neall VE (1991) Contrasting lithofacies architecture in ring plain deposits related to edifice construction and destruction, the Quaternary Stratford and Opunake Formations, Egmont volcano, New Zealand. Sediment Geol 74:71-88

Palmer BA, Alloway BV, Neall VE (1991) Volcanic debris-avalanche deposits in New Zealand: Lithofacies organization in unconfined, wet avalanche flows, In: Fisher RV, Smith GA (eds) Sedimentation in Volcanic Settings. Soc Sediment Geol (SEPM) Spec Publ 45:89-98

Palmer HS (1929) Volcanic mudflow in Java. Volcano Lett, no 253, Hawaiian Volcano Res Assoc

Paris R, Switzer AD, Belousova M, Belousov A, Ontowirjo B, Whelley PL, Ulvrova M (2014) Volcanic tsunami: A review of source mechanisms, past events and hazards in Southeast Asia Indonesia, Philippines, Papua New Guinea. Nat Hazards 70:447–470

Park J (1926) Morainic mounds on the Waimarino Plain near Ruapehu. Trans N Z Inst 56:382-383

Polanco E, Naranjo JA (2008) Collapso Holocene in the Callaqui volcano (37º55'S), Andes del Sur. Acta XVII Argentine Geol Cong July 2008:1157-1158

Ponomareva VV, Pevzner MM, Melekestsev IV (1998) Large debris avalanches and associated eruptions in the Holocene eruptive history of Shiveluch Volcano, Kamchatka, Russia. Bull Volcanol 59:490-505

Ponomareva VV, Melekestsev IV, Dirksen OV (2006) Sector collapses and large landslides on Late Pleistocene–Holocene volcanoes in Kamchatka, Russia. J Volcanol Geotherm Res 158(1-2):117-138

Pollack JB, Toon OB, Sagan C, Summers A, Baldwin B, Van Camp V (1976) Volcanic explosions and climate change: a theoretical assessment. J Geophys Res 81:1071-1083

Procter JN, Cronin SJ, Zernack AV (2009) Landscape and sedimentary response to catastrophic debris avalanches, western Taranaki, New Zealand. Sediment Geol 220:271-287

Quartau R, Ramalho RS, Madeira J, Santos R, Rodrigues A, Roque C, Carrara G, Brum da Silveira A (2018) Gravitational, erosional and depositional processes on volcanic ocean islands: Insights from the submarine morphology of Madeira Archipelago, Earth Planet Sci Lett 482:288-299

Ramirez CF (1988) The geology of Socompa volcano and its debris avalanche deposit, northern Chile. MSc diss, Open Univ, Milton Keynes, UK.

Rampino MR, Self S, Fairbridge RW (1979) Can rapid climatic change cause volcanic eruptions? Science 206:826-828

Ridley WI (1971) The origin of some collapse structures in the Canary Islands. Geol Mag 108:477-484

Rittmann A (1962) Volcanoes and their activity. Wiley, NY

Roberts, MA (2002) The geochemical and volcanological evolution of the Mt. Meru region, Northern Tanzania. Diss Univ Cambridge

Robin C, Camus G, Cantagrel JM, Gourgaud A, Mossand P, Vincent P, Aubert M, Dorel J, Murray JB (1984) Les Volcans de Colima (Mexique). Bull PIRPSEV, CNRS-INAG 87:1-98

Robin C, Mossand P, Camus G, Cantagrel JM, Gourgaud A, Vincent PM (1987) Eruptive history of the Colima volcanic complex (Mexico). J Volcanol Geotherm Res 31:99-113

1556 Rothpletz A (1889) Das Thal von Orotava auf Tenerife. Petermanns, Gotha

1557 Roverato M (2016) The Montesbelos mass-flow (southern Amazonian craton, Brazil): a
1558 Paleoproterozoic volcanic debris avalanche deposit? Bull Volcanol 78(7):49
1559
1560 Roverato M, Capra L (2013) Características microtexturales como indicadores del transporte y
1561 emplazamiento de dos depósitos de avalancha de escombros del volcán de Colima. Rev Mex
1562 Cien Geol 30:512-525
1563
1564 Roverato M, Capra L, Sulpizio R, Norini G (2011) Stratigraphic reconstruction of two debris
1565 avalanche deposits at Colima Volcano (Mexico): insights into pre-failure conditions and climate
1566 influence. J Volcanol Geotherm Res 207:33-46

1567 Roverato M, Cronin S, Procter J, Capra L (2015) Textural features as indicators of debris
1568 avalanche transport and emplacement, Taranaki volcano. Geol Soc Am Bull 127:3-18

1569 Ryabinin YN, Rodionov VN (1966) In: Vulkanizm gtubinnoe stroenie Zemli Tr Vsesoyuz Vulkanol
1570 Sovesh. (Volcanism and the Deep Structure of the Earth). Proc All-Union Volcanol Conf 3:56-60
1571 Nauka, Moscow
1572
1573 Samaniego P, Barba D, Robin C, Fornari N, Bernard B (2012) Eruptive history of Chimborazo
1574 volcano (Ecuador): A large, ice-capped and hazardous compound volcano in the Northern
1575 Andes. J Volcanol Geotherm Res 221-222:33-51

1576 Samaniego P, Valderrama P, Mariño J, van Wyk de Vries B, Roche O, Manrique N, Chédeville C,
1577 Liorzou, C, Fidel L, Malnati J (2015) The historical (218 ± 14 a BP) explosive eruption of
1578 Tutupaca volcano (Southern Peru). Bull Volcanol 77:51 https://doi.org/10.1007/s00445-015-
1579 0937-8
1580
1581 Satake K, Kate Y (2001) The 1741 Oshima-Oshima eruption: Extent and volume of submarine
1582 debris avalanche. Geophys Res Lett 28(3):427-430
1583
1584 Scott KM, Macías JL, Naranjo JA, Rodriguez S, McGeehin JP (2001) Catastrophic Debris Flows
1585 Transformed from Landslides in Volcanic Terrains: Mobility, Hazard Assessment, and Mitigation
1586 Strategies. U S Geol Surv Prof Pap 1630:1-59
1587
1588 Scott KM, Vallance JW, Kerle N, Macías JL, Strauch W, Devoli G (2005) Catastrophic precipitation-
1589 triggered lahar at Casita volcano, Nicaragua: occurrence, bulking and transformation. Earth Surf
1590 Process Landf 30:59–79
1591
1592 Sekiya S, Kikuchi Y (1889) The eruption of Bandai-san. Tokyo Imp Univ Coll Sci J 3(2):91-172
1593
1594 Schaffer FX (1926) Die Zehn-tausen Hugel von Tasikmalaja. Centralblatt Min Geol Paläont
1595 1926:207-209

1596 Shea T, van Wyk de Vries B (2008) Structural analysis and analogue modeling of the kinematics
1597 and dynamics of rockslide avalanches. Geosphere 4 (4):657–686

1598 Shimano T, Geshi N, Kobayashi T (2013) Geological map of Suwanosejima volcano. Geol Surv
1599 Japan, 1:20,000 map and explanatory text (in Jpn)

1600 Siebert L (1984) Large volcanic debris avalanches: characteristics of source areas, deposits, and
1601 associated eruptions. J Volcanol Geotherm Res *22*(3-4):163-197

1602 Siebert L (2002) Landslides resulting from structural failure of volcanoes. In: Evans SG, DeGraff JV
1603 (eds) Catastrophic landslides: effects, occurrence, and mechanisms. Geol Soc Am Rev Eng
1604 Geol XV:209-235

1605 Siebert L, Glicken H, Ui T (1987) Volcanic hazards from Bezymianny-and Bandai-type eruptions.
1606 Bull Volcanol 49(1):435-459

1607 Siebert L, Glicken H, Kienle J (1989) Debris avalanches and lateral blasts at Mount St. Augustine
1608 volcano, Alaska. Nat Geog Res 5:232-249

1609 Siebert L, Begét JE, Glicken H (1995) The 1883 and late prehistoric eruptions of Augustine
1610 volcano, Alaska, In: Ida Y, Voight B (eds) Models of magmatic processes and volcanic
1611 eruptions. J Volcanol Geotherm Res 66:367-395
1612
1613 Siebert L, Kimberly P, Pullinger CP (2004) The voluminous Acajutla debris avalanche from Santa
1614 Ana volcano, western El Salvador, and comparison with other Central American edifice-failure
1615 events. In: Rose, WI, Bommer JJ, Lopez DL, Carr MJ, Major JJ (eds) Natural Hazards in El
1616 Salvador. Geol Soc Am Spec Pap 375:5-23
1617
1618 Siebert L, Alvarado GE, Vallance JW, van Wyk de Vries B (2006) Large-volume volcanic edifice
1619 failures in Central America and associated hazards. In: Rose WI, Bluth GJS, Carr MJ, Ewert
1620 JW, Patino LC, Vallance JW, (eds) Volcanic Hazards in Central America. Geol Soc Am Spec
1621 Pap 412:1-26

1622 Siebert L, Vallance JW (2017) Large volume edifice failures in the Cascade Range of southern
1623 British Columbia to northern California. IAVCEI 2017 Scientific Assembly, Portland OR, Aug 14-
1624 18, 2017, abstr VH23A-181

1625 Silver E et al. (2005) Island arc debris avalanches and tsunami generation. EOS Trans Am
1626 Geophys Union 86:485-489
1627
1628 Silver E, Day S, Ward S, Hoffmann G, Llanes P, Driscoll N, Appelgate B, Saunders S (2009)
1629 Volcano collapse and tsunami generation in the Bismarck Volcanic Arc, Papua New Guinea. J
1630 Volcanol Geotherm Res 186(3–4):210-222
1631
1632 Stearns HT (1946) Geology of the Hawaiian Islands. Hawaii Div Hydrogr Bull 8:1-106
1633
1634 Stoopes GR, Sheridan MF (1992) Giant debris avalanches from the Colima Volcanic Complex,
1635 Mexico: implication for long runout landslides (> 100 km). Geology 20:299-302.

1636 Sutawidjaja IS, Suparman, Sitorus K (1996) Geologic map of Raung volcano, East Java. Volc Surv
1637 Indon 1:100,000 scale

1638 Tamura C, Hayakawa Y (1995) Reconstruction of the Sequence of the 1783 Asama Eruption from
1639 the Ancient Literature. J Geog 104(6):843-864 (in Jpn with Engl abstr)

1640 Taverne NMJ (1926) Vulkanstudien op Java. Vulk Seism Meded 7:78-83

1641 Taylor GAM (1974) Active volcanoes. In: Ford E (ed) Papua New Guinea Resource Atlas 6-7
1642 Jacaranda Press, Milton

Thompson BN (1965) White Island. In: Thompson BN, Kermode,LO (eds) New Zealand Volcanology—Northland, Coromandel, Auckland. N Z Geol Surv Handb Inf Ser 49: 68

Thouret J-C, Salinas R, Murcia A (1990) Eruption and mass-wasting-induced processes during the late Holocene destructive phase of Nevado del Ruiz volcano, Colombia. J Volcanol Geotherm Res 41(1–4):203–224

Tost M, Cronin SJ, Procter JN (2014) Transport and emplacement mechanisms of channelised long-runout debris avalanches, Ruapehu volcano, New Zealand. Bull Volcanol 76:881

Trofimovs J, Cas RAF, Davis BK (2004) An archean submarine volcanic debris avalanche deposit, Yilgarn Craton, western Australia, with komatiite, basalt and dacite megablocks: the product of dome collapse. J Volcanol Geotherm Res 138:111-126

Tsuchiya S, Sasahara K, Shuin S, Ozono S (2009) The large-scale landslide on the flank of caldera in South Sulawesi, Indonesia. Landslides 6(1):83-88

Ui T (1983) Volcanic dry avalanche deposits-identification and comparison with non-volcanic debris streams deposits. J Volcanol Geotherm Res 18:135-150

Ui T, Kawachi K, Neall VE (1986) Fragmentation of debris avalanche material during flowage – evidence from the Pungarehu Formation, Mount Egmont, New Zealand. J Volcanol Geotherm Res 27:255-264

Ui T, Yamamoto H, Suzuki-Kamata K (1986) Characterization of debris avalanche deposits in Japan. J Volcanol Geotherm Res 29:231-243

Vallance JW, Iverson RM (2015) Lahars and their deposits. In: Sigurdsson H, Houghton B, Rymer H, Stix J, McNutt S (eds) The encyclopedia of volcanoes, 2nd edn, pp 649–664

Vallance JW, Scott KM (1997) The Osceola mudflow from Mount Rainier: Sedimentology and hazard implications of a huge clay-rich debris flow. Geol Soc Am Bull 109(2):143-163

Vallance JW, Siebert L, Rose WI, Girón JR, Banks NL (1995) Edifice collapse and related hazards in Guatemala. In: Ida Y and Voight B (eds), Models of magmatic processes and volcanic eruptions. J Volcanol Geotherm Res 66:337-345

van Wyk de Vries B, Self S, Francis PW, Keszthelyi L (2001) A gravitational spreading origin for the Socompa debris avalanche. J Volcanol Geotherm Res 105:225-247

Verbeek RDM, Fennema R (1896) Geologische beschrijving van Java en Madoera. 2 vols, Stemler JG Amsterdam

Voight B, Glicken H, Janda RJ, Douglass PM (1981) Catastrophic rockslide avalanche of May 18. In: Lipman PW, Mullineaux DR (eds) The 1980 eruptions of Mount St. Helens, Washington: U S Geol Surv Prof Pap 1250:347-378

Voight B, Komorowski J-C, Norton GE, Belousov AB, Belousova M, Boudon G, Francis PW, Franz W, Heinrich P, Sparks RSJ, Young SR (2002) The 26 December (Boxing Day) 1997 sector collapse and debris avalanche at Soufriere Hills volcano, Montserrat. In: Druitt TH, Kokelaar BP (eds) The Eruption of Soufriere Hills Volcano, Montserrat, from 1995 to 1999. Geol Soc Lond Mem 21:363-407

Wadge G, Francis PW, Ramirez CF (1995) The Socompa collapse and avalanche event. J Volcanol Geotherm Res 66:309-336

Waitt RB, Begét JE (2009) Volcanic processes and geology of Augustine volcano, Alaska. U S Geol Surv Prof Pap 1762:1-78, 2 pl, scale 1:25,000

Waitz P (1906) Le Volcan de Colima. 10th Int Geol Congr, Field Trip Guide. chap 13:27

Waitz P (1932) Datos historicos y bibliograficos acerca del volcán de Colima. Mem Rev Soc Cient Antonio Alzate, Mex 53:349-384

Ward G (1922) White Island. N Z J Sci Technol 5:220-226

Ward SN, Day S (2003) Ritter Island Volcano—Lateral collapse and the tsunami of 1888. Geophys J Int 154:891-902

Watt SFL, Karstens J, Micallef A, Berndt C, Urlaub M, Ray M, Desai A, Sammartini M, Klaucke I, Böttner C, Day S, Downes H, Kühn M, Elger J (2019) From catastrophic collapse to multi-phase deposition: flow transformation, seafloor interaction and triggered eruption following a volcanic-island landslide. Earth Planet Sci Lett 517:135-147

Wilkinson P, Downie C, Cattermole PJ (1983) Quarter Degree Sheet 55. Geol Surv Tanzania, Arusha, scale 1:125,000

Wilkinson P, Mitchell JG, Cattermole PJ, Downie C (1986) Volcanic chronology of the Meru-Kilimanjaro region, northern Tanzania. J Geol Soc London 143:601–605

Williams H (1928) A recent eruption near Lassen Peak, California. Univ Calif Publ Geol Sci 17:241-263

Williams H (1941) Calderas and their origin. Calif Univ Publ Geol Sci 25:239-346

Williams H (1949) Geology of the Macdoel quadrangle. Calif Div Mines Bull 151:7-60

Williams H, McBirney (1968) An investigation of volcanic depressions: Part I – Geologic and geophysical features of calderas. NASA research grant NGR-38-033-012 progress report, 87 p

Williams H, McBirney (1979) Volcanology. Freeman, Cooper & Co San Francisco

Wolf F (1931) Der Vulkanismus II Band 2. Teil Alte Welt, Stuttgart

Worni R, Huggel C, Stoffel M, Pulgarín (2012) Challenges of modeling current very large lahars at Nevado del Huila volcano, Colombia. Bull Volcanol 74:309-324

Yamagishi H (1996) Destructive mass movements associated with Quaternary volcanoes in Hokkaido, Japan. Geol Soc Lond Spec Publ 110:267-279

Yamamoto T, Nakamura Y, Glicken H (1999) Pyroclastic density current from the 1888 phreatic eruption of Bandai volcano, NE Japan. J Volcanol Geotherm Res 90:191–207

Yamasaki, N (1898) Geology of volcano Yatsuga-dake and nearby volcanoes: Rep Imp Earthq Inv Com no. 20

Yoshida H (2016) Magnitude-frequency distribution of slope failures in Japan: Statistical approach to a true perspective on volcanic mega-collapses. In: Nemeth K (ed) Updates in volcanology – from volcano modelling to volcano geology, InTech, Croatia, pp 191-219

Yoshida H, Sugai T (2010) Grain Size Distribution of the Sediments from the 24 ka Sector Collapse of Asama Volcano, Japan. Trans Jpn Geomorph Union 31(2):193-201

Yoshimoto M, Ui T (1998) The 1640 sector collapse of Hokkaido Komagatake volcano, northern Japan. Bull Volcanol Soc Jpn 43:137-148 (in Jpn with Engl abstr)

Zernack AV, Procter JN (2020) Cyclic growth and collapse of stratovolcanoes. In: Roverato M, Dufresne A, Procter JN (ed) Volcanic Debris Avalanches: From Collapse to Hazard. Springer Book Series Advances in Volcanology, this volume

Zernack AV, Procter JN, Cronin SJ (2009) Sedimentary signatures of cyclic growth and destruction of stratovolcanoes: A case study from Mt. Taranaki, New Zealand. Sediment Geol 220(3-4):288-305

Zernack AV, Cronin SJ, Neall VE, Proctor JN (2011) A medial to distal volcaniclastic record of an andesitic stratovolcano: detailed stratigraphy of the ring-plain succession of south-west Taranaki, New Zealand. Int J Earth Sci 100:1937–1966

Zernack AV, Cronin SJ, Bebbington MS, Price RC, Smith IEM, Stewart RB, Proctor JN (2012) Forecasting catastrophic stratovolcano collapse: A model based on Mount. Taranaki, New Zealand. Geology 40 (11):983–986